Molecular Therapy
Nucleic Acids
Original Article

Exosomal DNA Aptamer Targeting α-Synuclein Aggregates Reduced Neuropathological Deficits in a Mouse Parkinson's Disease Model

Xiaoxi Ren,[1] Yun Zhao,[1] Fenqin Xue,[2] Yan Zheng,[3] Haixia Huang,[3] Wei Wang,[3] Yongchang Chang,[4] Hui Yang,[1] and Jianliang Zhang[1]

[1]Department of Neurobiology, Beijing Key Laboratory of Neural Regeneration and Repair, Beijing Institute of Brain Disorders, Key Laboratory for Neurodegenerative Disease of the Ministry of Education, Capital Medical University, Beijing 100069, China; [2]Core Facilities Center, Capital Medical University, Beijing 100069, China; [3]Department of Physiology, Capital Medical University, Beijing 100069, China; [4]Division of Neurobiology, Barrow Neurological Institute, St. Joseph's Hospital and Medical Center, Phoenix, AZ 85013, USA

The α-synuclein aggregates are the main component of Lewy bodies in Parkinson's disease (PD) brain, and they showed immunotherapy could be employed to alleviate α-synuclein aggregate pathology in PD. Recently we have generated DNA aptamers that specifically recognize α-synuclein. In this study, we further investigated the *in vivo* effect of these aptamers on the neuropathological deficits associated with PD. For efficient delivery of the aptamers into the mouse brain, we employed modified exosomes with the neuron-specific rabies viral glycoprotein (RVG) peptide on the membrane surface. We demonstrated that the aptamers were efficiently packaged into the RVG-exosomes and delivered into neurons *in vitro* and *in vivo*. Functionally, the aptamer-loaded RVG-exosomes significantly reduced the α-synuclein preformed fibril (PFF)-induced pathological aggregates, and rescued synaptic protein loss and neuronal death. Moreover, intraperitoneal administration of these exosomes into the mice with intra-striatally injected α-synuclein PFF reduced the pathological α-synuclein aggregates and improved motor impairments. In conclusion, we demonstrated that the aptamers targeting α-synuclein aggregates could be effectively delivered into the mouse brain by the RVG-exosomes and reduce the neuropathological and behavioral deficits in the mouse PD model. This study highlights the therapeutic potential of the RVG-exosome delivery of aptamer to alleviate the brain α-synuclein pathology.

INTRODUCTION

Parkinson's disease (PD) is the most prevalent form of synucleinopathies, which include PD, PD dementia (PDD), multiple system atrophy (MSA), and dementia with Lewy bodies (DLB). It is characterized by the abnormal deposition of the α-synuclein protein in the form of aggregates in neurons, leading to cell death and subsequent behavioral and motor deficits.[1] Currently, none of the existing therapies are able to slow down the neurodegeneration cascades that affect the diseased brain.[2] Therefore, to effectively delay or halt the progression of the disease, it is necessary to develop effective disease-modifying alternatives.

The tendency of α-synuclein to form aggregates is the key for its pathological function. α-Synuclein is a primarily cytosolic intracellular protein found at the presynaptic terminal,[3] and it is believed to have a role in vesicular transport and neurotransmitter release.[4] The α-synuclein aggregates, once taken up by acceptor cells, can act as seeds for further α-synuclein deposition within the recipient cells. This mechanism can explain the neurodegeneration pattern observed at different PD stages.[5,6] Thus, the processes of α-synuclein aggregation and fibrillation can be used as the therapeutic targets for the treatment of PD.[7]

Immunotherapy has emerged as a promising approach to target and clear the α-synuclein aggregate pathology in PD.[5,8] Although several agents have been identified to disrupt the α-synuclein aggregation,[9–11] the antibody-based immunotherapy is more appealing. The studies have shown that the antibodies against intracellular α-synuclein can inhibit α-synuclein aggregation and restore neurodegeneration in the mouse models.[12–14] Similarly, the immunotherapies against the other disease-causing proteins, such as Aβ,[15] tau,[16,17] SOD1,[18] and Huntingtin,[19] have been shown to decrease the protein aggregation and neurodegeneration. However, the later clinical trials of some antibodies, such as aducanumab, cannot reach their primary endpoint. Due to the protein nature, antibodies have their own weaknesses. For example, the antibodies do not easily get access to the intracellular target, and they are significantly immunogenic and more thermally unstable.[20] Therefore, there is an urgent need to develop antibody alternatives for application of the immunotherapy in PD. Aptamers are short, single-stranded DNA (ssDNA) or RNA molecules that can bind to a wide range of target proteins. They are

Received 9 May 2019; accepted 13 July 2019;
https://doi.org/10.1016/j.omtn.2019.07.008.

Correspondence: Jianliang Zhang, Department of Neurobiology, Beijing Key Laboratory of Neural Regeneration and Repair, Beijing Institute of Brain Disorders, Key Laboratory for Neurodegenerative Disease of the Ministry of Education, Capital Medical University, #10 Xitoutiao, Youanmenwai, Beijing 100069, China.
E-mail: jlzhang@ccmu.edu.cn

usually considered as "chemical antibodies." Aptamers have several advantages when compared with antibodies. First, they are neither immunogenic nor toxic molecules. Moreover, they have higher thermal stability and can maintain their structures over repeated cycles of denaturation and renaturation. In addition, they can even discriminate between different conformations of the same target protein,[21,22] although with some cross-interaction between the different forms of intrinsically disordered proteins.[23] Recently, we identified two DNA aptamers that specifically recognize α-synuclein. These aptamers can inhibit α-synuclein aggregation in a neuronal cell line and primary neurons, and reduce mitochondrial dysfunction and cell defects induced by α-synuclein overexpression.[24] Thus, it warrants further *in vivo* investigation of these aptamers for their ability to inhibit the α-synuclein aggregation and reduce neuropathological deficits.

Developing a safe and efficient vehicle to deliver an aptamer into the brain is still a challenging task. For siRNA delivery, three types of the delivery vehicle have been used, including viruses, polycationic polyethylenimine (PEI)-based nanoparticles, and liposomes.[25–27] However, these approaches are limited by stereotactic surgery, immune activation, toxicity problems, and non-specific targeting.[28,29] Interestingly, Alvarez-Erviti et al.[30] developed modified exosomes by fusing the neuron-specific rabies viral glycoprotein (RVG) peptide to the extra-exosomal N terminus of Lamp2b, an abundant membrane protein of the exosome, to allow the exosomes to enter the brain efficiently. The intravenous injection of RVG-modified exosomes, loaded with small interfering RNA (siRNA), into the normal mice leads to the targeted silencing of Beta-secretase1[30] or opioid receptor mu expression[31] in the brain. Furthermore, Cooper et al.[32] employed these nano-sized vesicles to deliver the α-synuclein siRNA into the mouse brain, and consequently reduced the intraneuronal α-synuclein aggregates and reversed the brain α-synuclein pathological condition, further highlighting its potential therapeutic value for neurological diseases.

In this study, we packaged the aptamers that recognized the α-synuclein fibrillar aggregates into the RVG-modified exosomes and investigated whether these exosomes were able to clear α-synuclein pathological aggregates in the cultured neurons and *in vivo* with the α-synuclein PFF-inoculated wild-type (WT) mice. It showed that in the primary neurons the RVG-exosomes loaded with aptamers significantly reduced the PFF-induced phosphorylated α-synuclein aggregates and rescued synaptic protein loss and neuron death. After systemic administration of these exosomes into the α-synuclein PFF-inoculated WT mice, the pathological α-synuclein aggregates in the brain were significantly reduced, and the associated motor dysfunction was rescued. In short, our study provided a potential therapeutic alternative via RVG-exosomes loaded with aptamers for treatment of PD.

RESULTS

Characterization of the DNA Aptamers and Selection of Aptamer for Therapy

Previous studies demonstrated that injection of the mouse α-synuclein preformed fibrils (PFFs) into young WT mice resulted in progressively recruiting endogenous mouse α-synuclein to form aggregates and further spreading of α-synuclein pathology.[33] Thus, targeting the α-synuclein aggregates appears to be a viable option to halt the initial step of synucleinopathies. Here we asked whether our previous selected aptamers could recognize the α-synuclein aggregates for PD treatment.

To characterize our selected aptamers, we first prepared the α-synuclein fibrillar aggregates *in vitro*. Specifically, the α-synuclein PFF was prepared in PBS with constant agitation from the purified recombinant human and mouse α-synuclein proteins. After separating the aggregated α-synuclein proteins from the soluble ones by ultracentrifugation, the majority of α-synuclein was present in the pellet (Figure 1A) in the form of high-molecular-weight aggregates as detected by western blot (Figure S1A). The morphology of the α-synuclein aggregates was further confirmed by transmission electron microscopy (TEM) analysis. The results showed human and mouse α-synuclein aggregates were large and broad with the ribbon-like fibrils. In contrast, the fibril-like structures were not detected in the soluble fraction of mouse α-synuclein (Figure 1B) or in the human α-synuclein monomer (data not shown). Taken together, the above data collectively confirmed that the human and mouse α-synuclein PFFs were both well-made.

Next, to test the aptamer capability to recognize the fibrillar α-synuclein, we performed the aptamer blotting along with the BSA control (Figure 1C). The results showed that the aptamers of F5R1 and F5R2 both bound to the human monomeric α-synuclein protein, but not BSA, as previously published.[24] Interestingly, both F5R1 and F5R2 had high affinities to human and mouse α-synuclein PFF. At the same time, F5R1 also bound slightly with the mouse monomeric α-synuclein protein. In contrast, F5R2 showed no binding signal to these monomers. We further confirmed the aptamer F5R2 did not react with the mouse monomeric α-synuclein in different amounts with serial dilutions (Figure S1B). Thus, for *in vivo* use, the aptamer F5R2 will not interfere with the endogenous α-synuclein in mice. Furthermore, we confirmed that aptamer F5R2 exhibited no reactivity with Aβ42 oligomers and its fibrils, although it bound slightly with the lysozyme fibrils (Figures S1C and S1D).

Because the interaction between α-synuclein PFF and α-synuclein monomers could seed progressive monomer aggregation,[34] we hypothesized that the binding of our aptamer to the α-synuclein PFF would prevent its interaction with the monomer, and thus inhibit the α-synuclein PFF-mediated progressive α-synuclein aggregation process. To test this hypothesis, we used thioflavin T (ThT) binding assay. Our result demonstrated that the presence of aptamer F5R2 significantly attenuates the α-synuclein PFF seeding process *in vitro* (Figure 1D). In the ThT binding assay for amyloid fibrils, the extent of ThT binding to amyloid fibrils depends on the accessibility of binding grooves or "channels" formed in fibril β sheets.[35] For α-synuclein, the presence of the aptamers, which could bind with the PFF, will probably interfere with ThT interacting with α-synuclein fibrils. In this scenario, we further employed the electron microscopy to assess

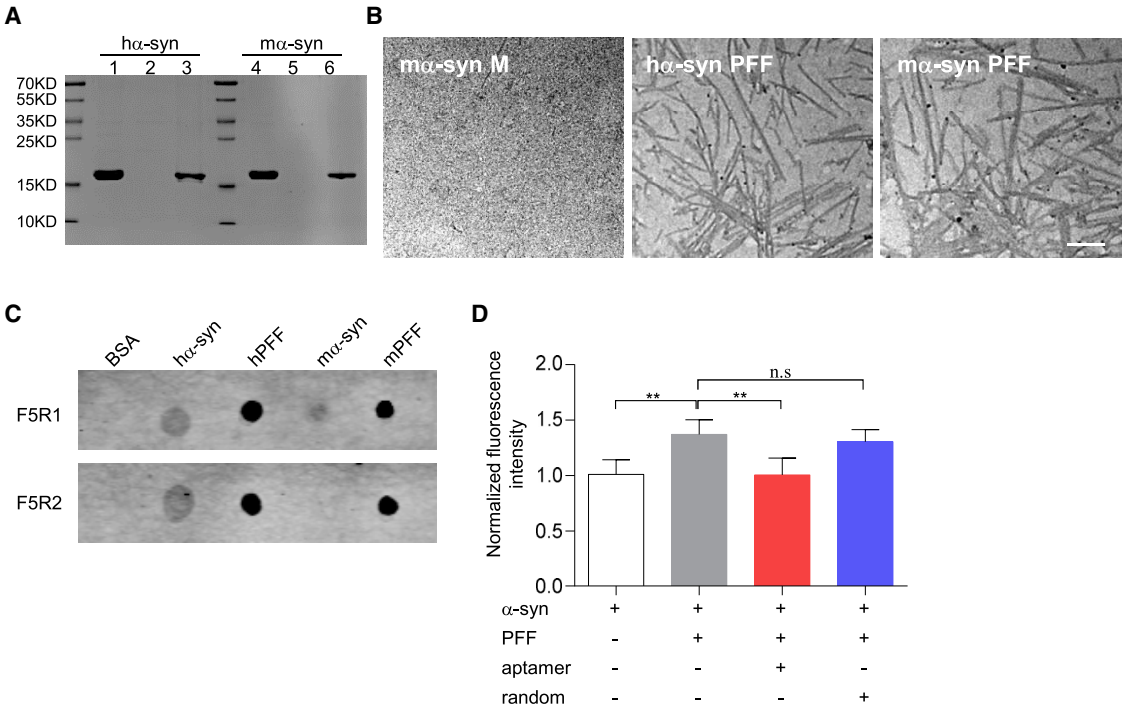

Figure 1. Characterization of the DNA Aptamers

(A) The α-synuclein PFF was prepared in PBS with constant agitation. After the α-synuclein fibril (pellet fraction) was separated from the α-synuclein monomer (supernatant fraction) by ultracentrifuge, the proteins were resolved by 10% SDS-PAGE and stained with Coomassie blue. Lane 1, purified human α-synuclein alone; lanes 2–3, supernatant and pellet fraction after human α-synuclein protein agitation; lane 4, purified mouse α-synuclein alone; lanes 5–6, supernatant and pellet fraction after mouse α-synuclein protein agitation. (B) TEM image of the α-synuclein PFF (pellet fraction) with the mouse monomeric α-synuclein (supernatant fraction) as a control. Scale bar, 200 nm. (C) Aptamer recognition capability assay by dot blotting. One-microgram samples (BSA, human monomeric α-synuclein, human α-synuclein PFF, mouse monomeric α-synuclein, mouse α-synuclein PFF) were respectively immobilized onto the nitrocellulose membrane for binding of each aptamer. (D) Aptamers could inhibit PFF-induced aggregation *in vitro*. Human α-synuclein monomer (20 μM) was incubated with 10% PFF in the presence of aptamer F5R2 (2 μM) at 37°C under shaking at 1,000 rpm. After shaking for 24 h, the amyloid formation was monitored by measuring ThT fluorescence. Values are presented as mean ± SD. One-way ANOVA followed by Tukey's post hoc test (n = 6 independent experiments for each group), **$p < 0.01$.

the effect of aptamer F5R2 on this process to exclude this possibility (Figure S2).

Based on the aptamer recognition capability and its capacity to inhibit α-synuclein PFF seeding efficiency, we chose the aptamer F5R2 for the subsequent therapy in the mouse α-synuclein PFF model of the sporadic PD because this aptamer could bind to the aggregated α-synuclein without interfering with the endogenous mouse α-synuclein, potentially leading to the inhibition of α-synuclein aggregation in the mice.

Characterization of RVG-Exosomes and Its Delivery of the Aptamer into Neuronal Cells

To facilitate delivery of the aptamer into the mouse brain, we generated the neuron-specific exosomes according to the previous publication.[30] The RVG-modified exosomes were characterized by TEM and western blotting. The TEM data showed that the exosomes presented normal morphological characteristics, with an average diameter of approximately 100 nm, and that each vesicle was surrounded by a double-layer membrane (Figure 2A); western blot analysis showed that the exosome marker protein Alix could be detected in a dose-dependent manner with increasing sample loading (Figure S3D). These characteristics indicated that the exosome properties were not affected by the RVG modification. Further immunoprecipitation results suggested that RVG-positive exosomes account for around 18% of the total ones (Figure S3C).

Next, we investigated the loading of aptamers into RVG-modified exosomes using the PEI transfection protocol. Alexa 594-labeled aptamer was used for fluorometric detection after transfection, and the amount of encapsulated aptamers was assayed after ultracentrifugation. The fluorescent plate reading data showed that transfection for 2 h resulted in the greatest retention of aptamer (Figure S4A). This was further confirmed by confocal microscope, showing that most of the exosomes were co-localized with aptamers (Figure S4B). Furthermore, the PEI transfection did not substantially alter the physical properties of the RVG-exosomes loaded with aptamers (Figure S3B). For the subsequent loading of aptamers into exosomes, unless otherwise noted, transfection with PEI for 2 h was used.

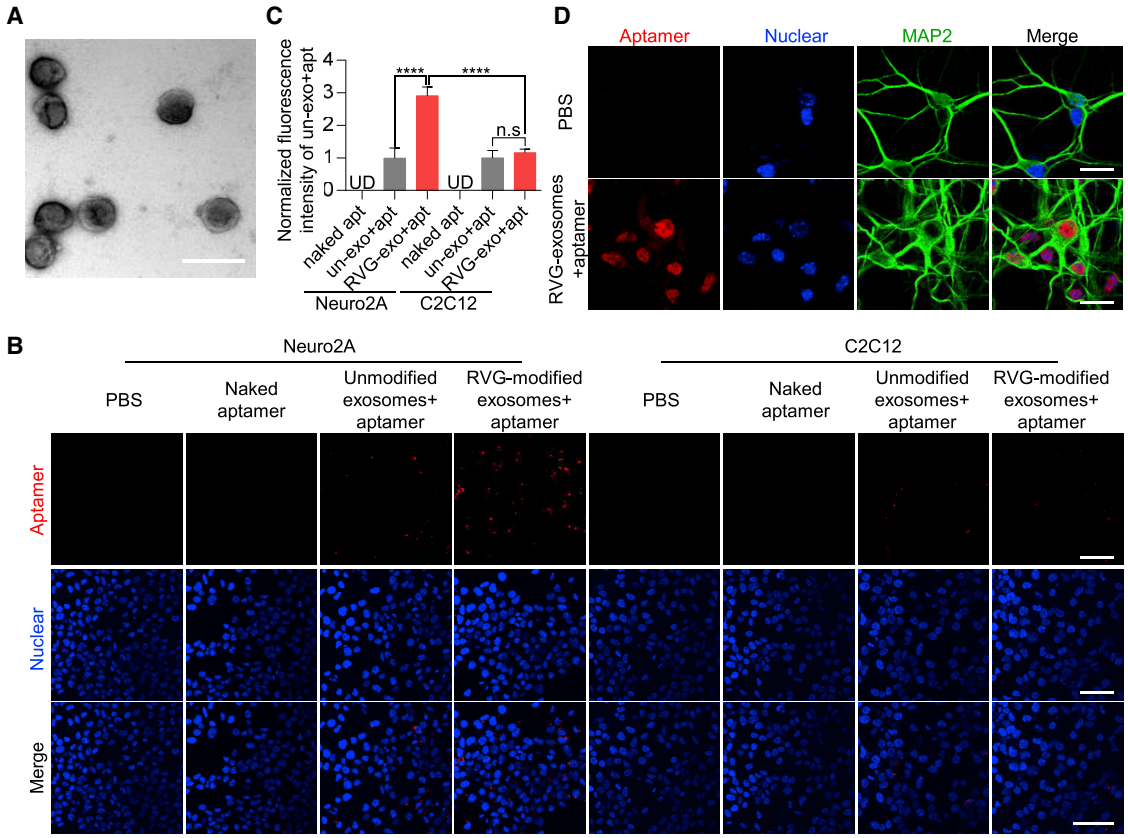

Figure 2. Characterization of RVG-Exosomes and Their Delivery of Aptamer F5R2 into Neuronal Cells

(A) TEM image of the RVG-exosomes purified from the culture medium of HEK293T cells. Scale bar, 200 nm. (B) Confocal microscopy images, showing the delivery of aptamers F5R2 into the neuronal cells by RVG-exosomes. Vehicle (columns 1 and 5), naked aptamer F5R2-Alexa 594 (columns 2 and 6), aptamer F5R2-Alexa 594-loaded unmodified exosomes (columns 3 and 7), and aptamer F5R2-Alexa 594-loaded RVG-exosomes (columns 4 and 8). Scale bars, 25 μm. (C) Bar graph quantitation of the fluorescence intensity of the packaged aptamers. For each group, the fluorescence intensity was measured with six independent chamber slides (three fields per slide were counted). The aptamers packaged into the cells were expressed as fluorescence intensity and were normalized to the group of the unmodified exosomes + aptamer for statistical comparisons. Values are presented as mean ± SD. One-way ANOVA followed by Tukey's post hoc test, ****$p < 0.0001$. (D) Confocal microscopy images of fluorescently labeled aptamer F5R2 in primary neurons. The MAP2 (green) was used as the marker of neurons. Scale bars, 25 μm.

To confirm RVG-exosomes can deliver aptamers into neurons, we selected the Neuro2A cell line as the recipient cells, with the skeletal muscle cell C2C12 as the control. First, after confirming the exosomes could deliver the aptamers into the Neuro2A cells at 24 h (Figure S4C), the confocal image showed that the fluorescence intensity in the cells was increased with time, suggesting that the aptamer uptake efficiency was positively correlated with the incubation time. The incubation for 48 h resulted in the highest exosome uptake efficiency (Figures S4D and S4E). Next, to confirm the RVG-exosome targeting capabilities, Neuro2A cells were treated with the RVG-exosomes loaded with the aptamers for 48 h. The result showed that these cells were fluorescently detectable under fluorescence confocal microscopy; however, the cells untreated or treated with aptamer alone or WT-exosome alone had very weak fluorescent signals (Figure 2B). In contrast, RVG-exosomes could not efficiently enter the non-neuronal C2C12 cells. This is likely due to that the cell line does not have the RVG peptide receptor on their membrane (Figures 2B and 2C). In addition, both cell lines could tolerate the aptamer-loaded exosomes treatment, as reflected by lactate dehydrogenase (LDH) assay and 3-(4,5-dimethylthiazol-2-yl)-2,5-diphenyltetrazolium bromide (MTT) assay (Figure S5).

To further confirm the aptamer-delivery effect of RVG-exosomes in the primary neurons, we treated the mouse primary neurons with the RVG-exosomes loaded with Alexa 594-labeled aptamers for 24 h. The confocal scanning data showed that the aptamers could be delivered into the primary neurons through the RVG-exosomes (Figure 2D).

Taken together, these data clearly demonstrated that the RVG peptide incorporation into the exosomal membrane preferentially guides the exosomes to neuronal cells, allowing for efficient delivery of the aptamer into the neuronal recipient cells.

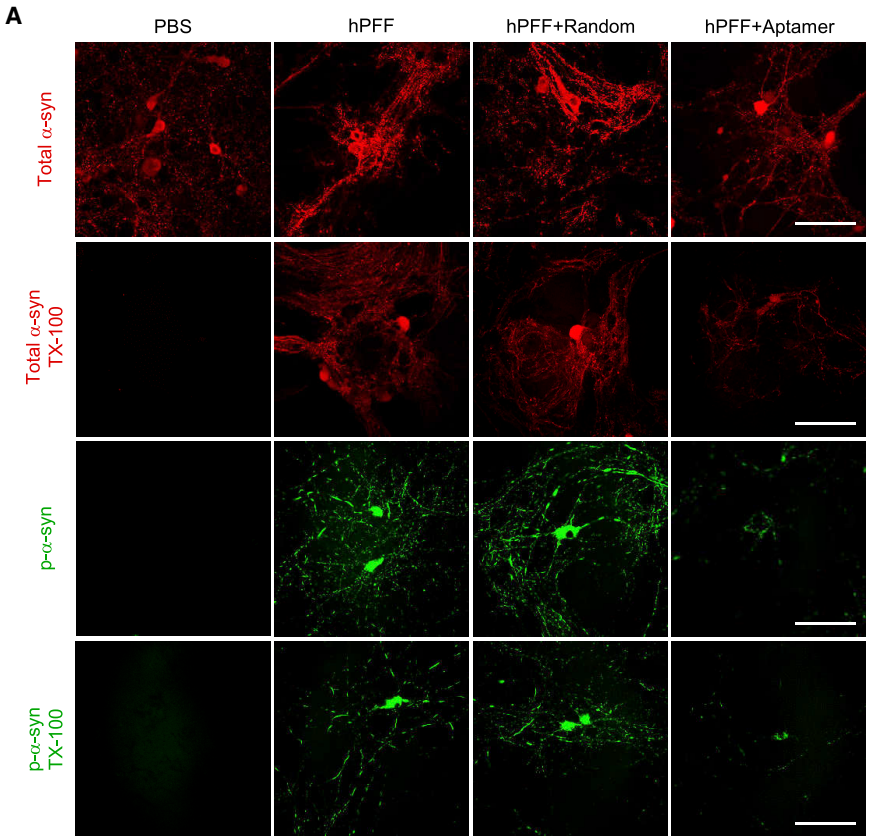

Figure 3. Aptamers Could Reduce PFF-Induced Insoluble Pathologic Aggregates in Primary Neurons

Primary neurons were treated with RVG-exosomes loaded with the aptamer or random DNA sequence at 6 DIV and then treated with PBS or PFF at 7 DIV. (A) At 14 DIV, neurons were fixed with 4% PFA with or without 1% TX-100 to extract soluble proteins. Confocal microscopy was used to monitor endogenous mouse α-synuclein (red) and p-α-synuclein (green) in neurons. Scale bars, 25 μm. (B) Neurons were lysed sequentially in 1% TX-100 (TX-soluble) followed by 2% SDS (TX-insoluble) at 21 DIV, and western blotting was used to analyze the level of mouse α-synuclein and p-α-synuclein in the lysates. One-tenth dose of aptamer-loaded RVG-exosomes was applied as the low-dose treatment group, and similarly the 1/10 random DNA sequence group was also set as the negative control. The β-actin was served as the loading control. (C) Bar graph quantitation of the protein level of endogenous mouse α-synuclein from the TX-insoluble fraction. Values are presented as mean ± SD. One-way ANOVA followed by Tukey's post hoc test (n = 3 independent experiments for each treatment), *$p < 0.05$, **$p < 0.01$ compared with the group treated with a random DNA sequence. (D) Bar graph quantitation of the protein level of p-α-synuclein from the TX-insoluble fraction. Values are presented as mean ± SD. One-way ANOVA followed by Tukey's post hoc test (n = 3 independent experiments for each treatment), *$p < 0.05$, **$p < 0.01$ compared with the group treated with a random DNA sequence.

The Aptamers Reduced PFF-Induced Insoluble Pathologic Aggregates in the Mouse Primary Neurons

After confirming that aptamers could be efficiently delivered into the neuronal cells through RVG-exosomes, we then assessed whether aptamers packaged in the RVG-exosomes could inhibit the α-synuclein aggregation and suppress pathological changes caused by PFF in the primary neurons. To achieve this goal, we delivered aptamers to the mouse primary neurons via the RVG-exosomes 24 h before the human α-synuclein PFF treatment. On the 7th day after PFF treatment, in the PBS-treated group, endogenous mouse α-synuclein diffusely distributed in cells. However, this distribution pattern was significantly disturbed in the PFF-treated neurons because of the recruitment of endogenous mouse α-synuclein into aggregates (Figure 3A, upper panels; Figure S6). Then, we extracted neurons using the fixation buffer containing 1% Triton X-100 (TX-100) to determine whether these α-synuclein aggregates were insoluble. Under this experimental condition, endogenous mouse α-synuclein in the PBS group was completely extracted, whereas the PFF-treated group showed TX-100-insoluble aggregates. Interestingly, addition of the RVG-exosomes loaded with the aptamer reduced the extent of the fibrillar aggregation. In contrast, random DNA sequence had no effect on α-synuclein aggregation pattern (Figure 3A, upper panels). Thus, the aptamer delivered into the primary neurons inhibited the formation of the α-synuclein insoluble aggregates induced by PFF.

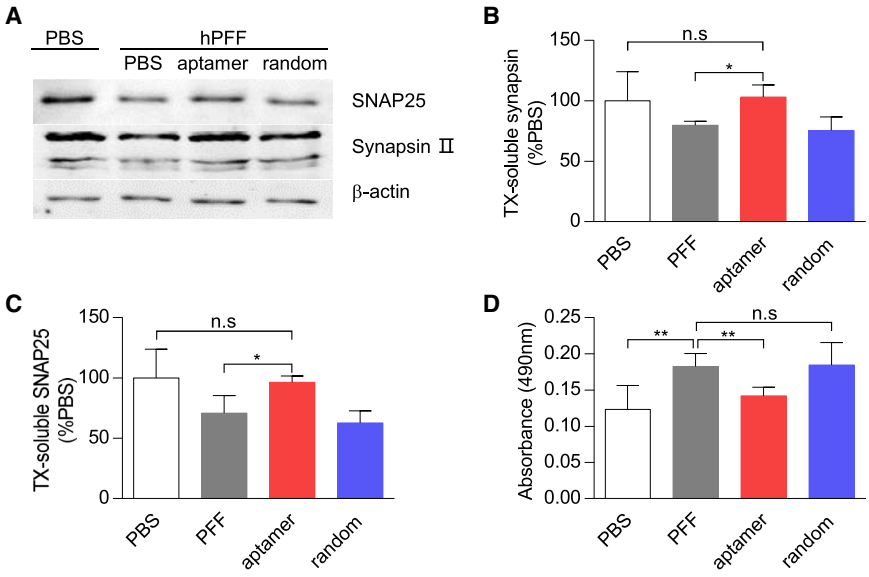

Figure 4. Aptamers Reduced α-Synuclein PFF-Induced Synaptic Loss and Neuron Death

(A) Primary neurons were similarly treated as in Figure 3. At 21 DIV, proteins of SNAP25 and synapsin II in TX-soluble fraction were analyzed by western blot. β-Actin was served as the loading control. (B and C) Bar graph quantitation of the protein level of synapsin II (B) and SNAP25 (C) from the TX-soluble fraction. Values are presented as mean ± SD. One-way ANOVA followed by Tukey's post hoc test (n = 3 independent experiments for each treatment), *p < 0.05. (D) Bar graph quantitation of the LDH level in culture media at 21 DIV. Values are presented as mean ± SD. One-way ANOVA followed by Tukey's post hoc test (n = 6 independent experiments for each group), **p < 0.01.

In addition, previous studies showed that phosphorylation of the serine residue at the 129 position of α-synuclein (p-α-syn) is a marker of intracellular α-synuclein pathology because exogenously added PFF lacks this modification.[36] We further tried to confirm the presence of pathological α-synuclein by measuring the phosphorylation level of Ser129 of the α-synuclein protein. In the PBS-treated group, we did not observe the presence of p-α-syn, whereas in the PFF-treated group, the presence of p-α-syn was clearly visible in the aggregated state. Furthermore, the p-α-syn-positive inclusions were still remarkably detected even after TX-100 treatment, but not in the PBS-treated group. Notably, this pathology was significantly reduced by the aptamer treatment, but not by a random DNA sequence treatment (Figure 3A, lower panels), suggesting aptamer could inhibit PFF to recruit endogenous mouse α-synuclein into p-α-syn-positive inclusions. Thus, these results demonstrated that the aptamer delivered into the primary neuron via RVG-exosomes reduced α-synuclein Ser129 phosphorylation level caused by PFF.

Furthermore, the above findings were bolstered by western blotting analysis. The soluble and insoluble α-synuclein fractions were prepared after sequentially extracting neurons in 1% TX-100 followed by 2% SDS. The western blotting results showed that TX-insoluble α-synuclein was present in the group treated with PFF (Figure 3B), suggesting that mouse endogenous α-synuclein was recruited into Lewy body (LB) or Lewy neurite (LN)-like aggregates by PFF. Particularly, the higher-molecular-weight α-synuclein bands detected by antibody to α-synuclein or p-α-syn in the TX-insoluble fractions of PFF-treated cultures are also evident, likely corresponding to phosphorylated, multimeric, or other posttranslational modified forms of α-synuclein (Figure 3B). Notably, those aggregates in TX-insoluble preparation were dramatically reduced by aptamer treatment to 60.36% ± 6.37%, when compared with the group treated with a random DNA sequence, and one-tenth dose of the aptamer treatment reduced to 69.74% ± 13.00% (Figures 3B and 3C). At the same time, TX-insoluble p-α-synuclein fraction was also significantly reduced to 70.75% ± 4.43%, and one-tenth dose of the aptamer treatment reduced to 86.37% ± 1.72% (Figures 3B and 3D). Collectively, these data further demonstrated that aptamers could reduce PFF-induced insoluble pathologic aggregates.

Aptamers Rescued the Synaptic Protein Loss and Neuron Death Induced by PFF

Previous studies demonstrated PFF-induced α-synuclein aggregates might cause the synaptic protein loss and neuron death.[36,37] Here, we further tested whether the aptamers could reduce the synaptic protein loss and protect against the neuron death. Indeed, whereas PFF treatment resulted in a loss of the synaptic protein of synapsin II and SNAP25, addition of the aptamers clearly preserved their protein level (Figures 4A–4C). Moreover, the aptamer treatment significantly reduced the LDH level caused by the PFF treatment. This effect was not observed in the group treated with a random DNA sequence (Figure 4D). Therefore, the aptamer could prevent the synaptic protein loss and potentially rescue the neuron death induced by PFF.

RVG-Exosomes Delivered Aptamers into the Mouse Brain

To determine whether aptamers could also reduce α-synuclein aggregation and its associated neuropathology *in vivo*, first we need to know whether the aptamers can be efficiently delivered into the brain tissues by RVG-exosomes. For this purpose, the CellVue Claret-labeled RVG-exosomes loaded with Alexa 594-labeled aptamers were intraperitoneally injected into the C57BL/6J mice (2–3 months old) with aptamer alone as the control. Twenty-four hours later, the mice were anesthetized, perfused, and the brain slides were scanned by confocal microscopy. The images indicated that the purple RVG-exosomes and red Alexa 594 were detectable in the brain cortex and midbrain, and no fluorescence was detected in the control group (Figures 5A and 5B). This suggests that the aptamer was delivered into the brain efficiently by the RVG-exosomes, but not by the unmodified exosomes (Figures S7A and S7B). In addition, the immune responses analysis further indicated that the treatment with

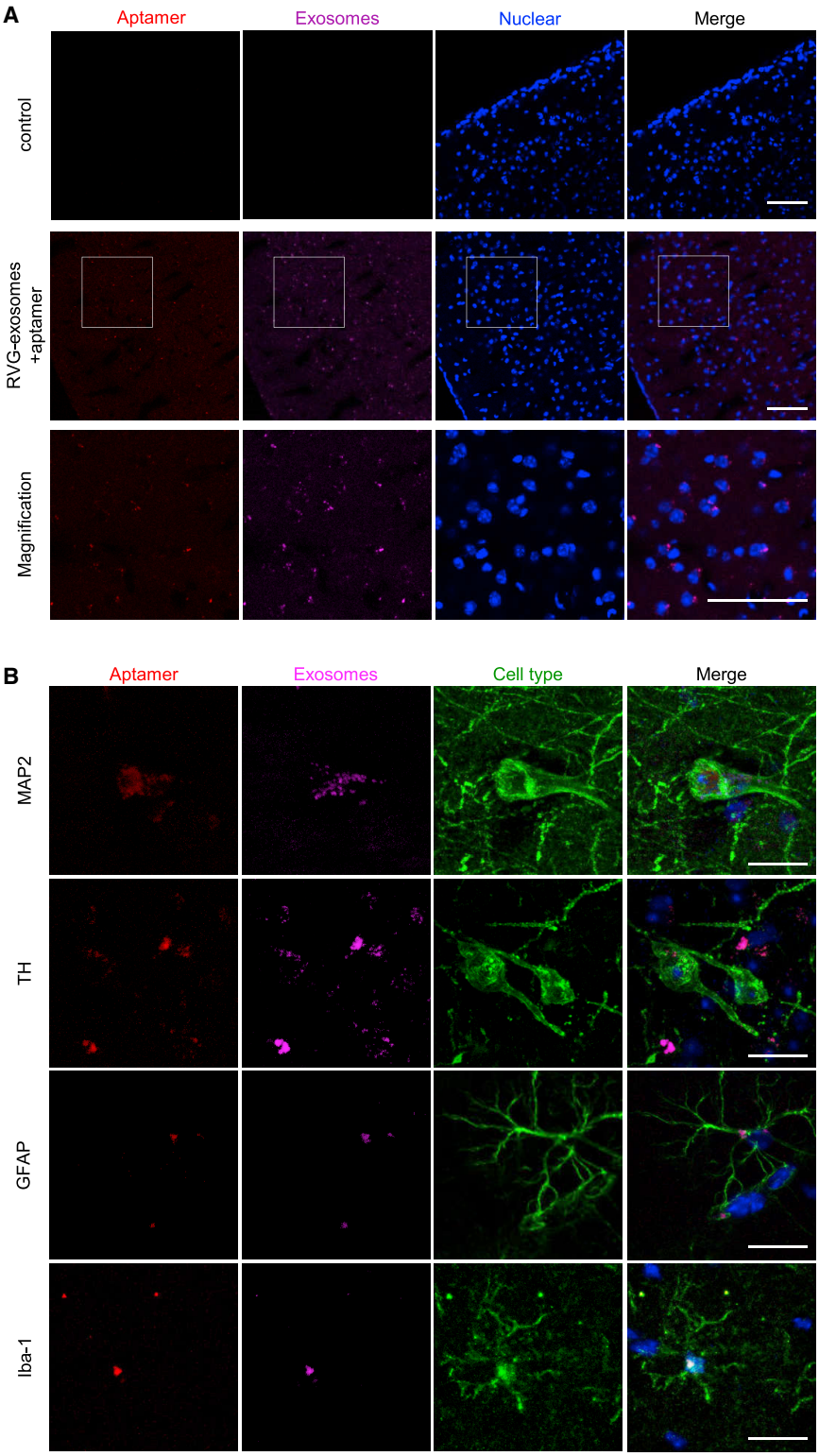

Figure 5. RVG-Exosomes Delivered Aptamers Efficiently into the CNS in Mice

CellVue Claret-labeled RVG-exosomes loaded with Alexa 594-labeled aptamer F5R2 were administered into mice by intraperitoneal injection. Mice were anesthetized and sacrificed 24 h after the injection, and the brain was sectioned at a thickness of 40 μm. (A) Confocal microscopy images show the delivery of aptamers F5R2 (red) into the brain cortex by RVG-exosomes (purple). Scale bars, 75 μm. (B) Sections were stained with antibodies (anti-MAP2, anti-TH, anti-GFAP, and anti-Iba-1) to localize the aptamers F5R2/RVG-exosomes with different cells in the mouse midbrain.

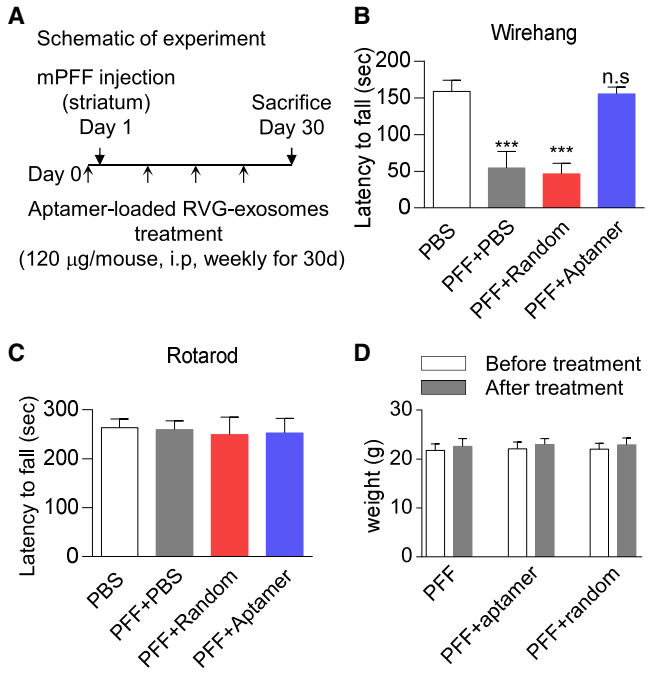

Figure 6. Aptamers Rescued the Mouse Grip Strength Loss Induced by PFF

(A) Schematic representation of experimental design. (B and C) Wire hang (B) and rotarod task (C) performance of mice at 30 days post PFF injection with aptamer-loaded RVG-exosomes treatment. RVG-exosomes group loaded with a random DNA sequence was used as the control. Values are presented as mean ± SD. One-way ANOVA followed by Tukey's post hoc test (n = 12 mice per group), ***$p < 0.001$; n.s., not significant, compared with RVG-exosomes group loaded with a random DNA sequence. (D) The weights of mice were measured before and after aptamer-loaded RVG-exosome treatment, to verify whether the treatment could be tolerated by animals. Values are presented as mean ± SD. Two-way ANOVA followed by Tukey's post hoc test (n = 12 mice per group). There was no significant difference between each group.

RVG-exosomes loaded with aptamers did not induce significant immune responses *in vivo* (Table S1).

To identify the cell types in the brain with the delivered aptamers, we co-stained the brain slides with different biomarkers. Confocal images showed that the aptamer and RVG-exosomes were co-localized in the neurons, microglia, and astrocytes in the midbrain (Figure 5B), implying that the aptamer indeed was delivered into the brain cells whose membrane contains the neuronal nicotinic acetylcholine receptors. Taken together, these results suggested that RVG-exosomes could deliver aptamers into the mouse brain by intraperitoneal injection. This method was selected for the further evaluation of aptamer therapeutic effects *in vivo*.

Aptamers Rescued the Mouse Grip Strength Loss Induced by PFF and Reduced the Accumulation of the Pathological α-Synuclein Aggregates *In Vivo*

After demonstrating that the aptamer could be delivered to the mouse brain by RVG-exosomes and reduce pathological α-synuclein aggregates in the primary neurons, we then asked whether aptamers could reduce the α-synuclein pathology *in vivo*. To this end, we used the mouse α-synuclein PFF model of the sporadic PD, and the RVG-exosomes loaded with the aptamer were intraperitoneally injected into the C57BL/6J female mice (2–3 months old). Twenty-four hours later, mouse α-synuclein PFF was injected into the right striatum of the mice. During the next 4 weeks, the mice were given RVG-exosomes loaded with aptamer weekly. The RVG-exosomes loaded with random DNA sequence were given to the mice as the negative control (Figure 6A). Thirty days after PFF injection, the efficacy of the aptamer therapy was assessed with the behavioral and histological analyses.

To assess the effect of aptamers on the motor function, we performed the wire hang test and rotarod test. The wire hang test measures the time until the animal loses its grip. The results demonstrated that non-PFF-treated mice were holding on to the wire for 158 s on average, whereas the PFF-treated mice were able to hold on only around 54 s. Notably, the aptamer treatment significantly enhanced the time of the mice on the wire (around 150 s). In contrast, this effect was not observed in the group treated with a random DNA sequence (Figure 6B). For the rotarod task, the mice performance exhibited no difference between the naive and PFF-treated group, so it was practically impossible to see the effect of aptamer on their rotarod performance at this time point (Figure 6C). In addition, the mice tolerated the aptamer treatment well, because they gained weight normally and appeared healthy until the termination of the experiment (Figure 6D). Collectively, these data indicated that the aptamer could rescue the grip strength loss induced by PFF.

Next, we determined whether aptamers could reduce the pathological α-synuclein aggregates in the brain. In the control group treated with a random DNA sequence, the aggregation of p-α-syn was primarily detected in the ipsilateral cortex, although the p-α-syn signals were also detected on the contralateral side. Noteworthy, in the aptamer-treated group, the aggregation of p-α-syn in the ipsilateral and contralateral cortex was significantly reduced (Figures 7A–7C). Moreover, for the substantia nigra, in the group treated with a random DNA sequence, the aggregation of p-α-syn was detected only in the ipsilateral substantia nigra, but not in the contralateral substantia nigra. This observation is consistent with a previous report.[37] Importantly, the aptamer treatment significantly depressed the aggregation of p-α-syn in the ipsilateral substantia nigra (Figures 7D and 7E). Thus, the administration of aptamers reduced the pathology in this α-synuclein PFF mouse model of PD.

In addition, because the aptamers also could be delivered into the brain microglia and astrocytes, the quantity and morphology of microglia and astrocyte cells were also assessed with glial fibrillary acidic protein (GFAP) and Iba1 antibodies. It was found that there was no significant difference in the extent of astrogliosis and microgliosis between the random DNA sequence- and aptamer-treated mice (Figures 7F–7H), implying the mild brain neurodegeneration in the mice at this time point.

Taken together, these data showed that aptamers could reduce pathologic α-synuclein aggregation *in vivo* and ameliorated the motor dysfunction in our PD mouse model.

DISCUSSION

Our study demonstrated the aptamers delivered by RVG-exosomes reduced the pathological α-synuclein aggregates *in vitro* and in the PD models, and ameliorated the mouse behavioral deficits. The aptamers loaded into the RVG-exosomes by transfection could be preferentially targeted into neuronal cells and the mouse primary neurons. In the primary neurons treated with α-synuclein PFF, the aptamers were capable of retarding PFFs recruiting endogenous α-synuclein into pathologic aggregates, consequently leading to rescuing synaptic protein loss and mitigating neuron death caused by pathologic α-synuclein. In the WT mice subjected to the intrastriatal injection of α-synuclein PFF, the aptamer treatment decreased the pathological α-synuclein aggregates in the brain, particularly in the cortex and midbrain, which are important areas affected by α-synuclein inclusions in PD (Figure 8). Taken together, our study highlighted the therapeutic potential of the RVG-exosome delivery of aptamers to slow down or even halt α-synuclein pathological conditions.

Accumulating studies suggest that during the PD development, the misfolded α-synuclein proteins act as a seed, recruiting endogenous α-synuclein into aggregates. Accumulation of α-synuclein aggregates and subsequent amyloid chains results in generation of more seeds, which cause accelerated accumulation of more pathological aggregates within cells and propagation between cells; consequently, the process is hypothesized to be relevant to the PD development. Thus, the aggregated α-synuclein might be worth targeting. It has been demonstrated that Syn303, a species-independent monoclonal antibody against the α-synuclein inclusions, can reduce pathological α-synuclein aggregates in primary neurons.[38,39] Likewise, this antibody also retarded the LB or LN pathology and improved motor impairments in the mouse α-synuclein PFF model, by targeting the α-synuclein PFF and consequently limiting its recruitment of endogenous mouse α-synuclein into pathologic aggregates and blocking the cell-to-cell transfer of α-synuclein aggregates.[37] Given the inherent weakness of the antibodies in clinical use, it is urgent to find the antibody alternatives for application of the immunotherapy in PD. At present it seems that aptamers are very appealing.[20]

In our recent work, by systematic evolution of ligands by exponential enrichment (SELEX) on human recombinant α-synuclein, we obtained two aptamers (named as F5R1 and F5R2), which were found to specifically target the human α-synuclein with high affinities.[24] In this study, we further found that these two aptamers could recognize the human and mouse PFF. Aptamer F5R1 still had a slight binding capacity with the mouse monomeric α-synuclein, whereas F5R2 absolutely did not cross-react with it. For directly blocking the α-synuclein PFF initial seeding effect without interfering with endogenous α-synuclein in mice, aptamer F5R2 would be a good choice. Thus, the aptamer F5R2 was chosen in our current study.

The brain-specific targeted exosomes showed the potential to serve as a highly efficient strategy for transferring aptamers into the CNS. Despite the recent advance in delivering nucleic acids, it is still challenging to target these cargos to specific tissues or cell types while avoiding immunogenicity. It is particularly a real problem in the case of chronic disease conditions, such as PD, that require a long period of treatment. Exosomes are naturally occurring nano-sized vesicles (30–120 nm) secreted by numerous cell types and have attracted much attention as drug delivery vehicles in recent years, because exosomes may have an immune-privileged status that can efficiently decrease drug clearance and show any toxicity.[40,41] Further, to confer the exosomes with the brain-targeting capability, the exosomal outer membrane protein, Lamp2b, was engineered to be fused with the neuron-specific RVG peptide, leading to the RVG-modified exosomes with the potential to deliver the nucleic acids into the cells that express the neuronal nicotinic acetylcholine receptor.[30,32] The RVG-exosomes purified from HEK293T cells had been employed to deliver siRNAs to downregulate opioid receptor Mu and inhibited morphine relapse in mice.[32] In this study, we constructed a plasmid expressing the fusion protein of RVG-Lamp2b, and employed HEK293T cells as donor cells to obtain the exosomes expressing RVG on the membrane surface. The acquired RVG-exosomes showed normal morphological characteristics after modification, and the DNA aptamer loading was conducted efficiently by transfection. We demonstrated that these exosomes delivered aptamers into the Neuro2A cells and primary neurons, further suggesting that we have the right tool for the aptamer delivery to neurons.

LBs are the key pathological feature of PD and contain large amounts of α-synuclein aggregates. It has been demonstrated that injection of mouse α-synuclein PFF into non-transgenic (Tg) mice can recruit endogenous α-synuclein to form LB or Lewy-like aggregates and propagate this pathological feature in mice.[37] Thus, in this study, we selected the α-synuclein PFF mouse model to determine whether aptamer-loaded RVG-exosomal therapy can impact on the level of α-synuclein aggregates *in vivo*. As for the RVG-exosome administration route, normally an intravenous injection could yield rapid absorption and increase the therapeutic effect. However, in our study we had to repeat the RVG-exosomes administration to the mice many times. In this scenario, we considered that the intraperitoneal injection was more preferable. Indeed, it was confirmed that the aptamers could also be efficiently delivered into the brain by intraperitoneal injection, and this treatment with RVG-exosomes loaded with aptamers did not induce significant immune responses *in vivo*. As for the aptamer therapeutic effect, consistent with our findings that aptamer F5R2 could inhibit the α-synuclein PFF-mediated α-synuclein aggregation process *in vitro*, systemic administration of the aptamer decreased the pathological α-synuclein aggregates in the cortex and substantia nigra in the WT mice injected with mouse α-synuclein PFF. Additionally, the aptamers also rescued the mouse-weakened grip strength induced by the PFF under our experimental condition. Notably, over the short experimental period, the mice did not demonstrate any obvious signs of the dopaminergic neuron loss,[33] so it will be of importance for the future studies to perform detailed clinical

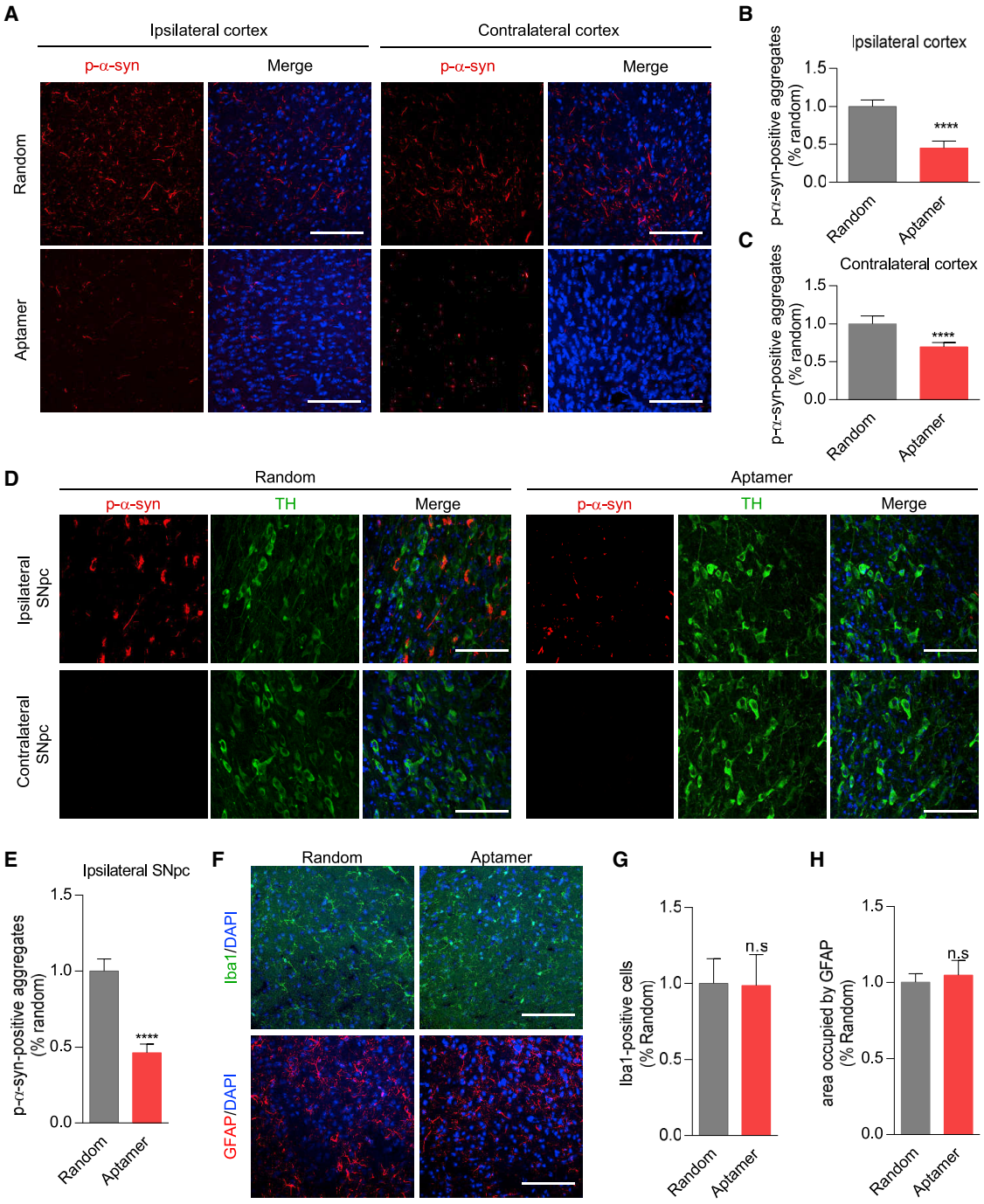

Figure 7. Aptamer Could Reduce PFF-Induced Aggregation of α-Synuclein *In Vivo*

(A) Immunohistochemistry for measuring the p-α-synuclein in the cortex. Mouse α-synuclein PFF injection led to α-synuclein aggregates in the ipsilateral and contralateral prefrontal cortex, and the aptamer treatment significantly reduced the pathology in these regions. Scale bars, 75 μm. (B and C) Bar graph quantitation of the p-α-synuclein level in the ipsilateral cortex (B) and contralateral cortex (C). For each treatment, the fluorescence intensity was measured with eight mice (three slides per mouse were counted). The phosphorylated α-synuclein aggregates were expressed as fluorescence intensity, and the intensity in the aptamer-treated group was normalized to the group treated with a random DNA sequence for statistical comparisons. Values are presented as mean ± SD. Student's t test, ****$p < 0.0001$, compared with RVG-exosomes group loaded with a random DNA sequence. (D) Confocal microscopy images to show the effect of aptamer F5R2 on the p-α-synuclein accumulation in the ipsilateral substantia nigra. Anti-TH antibody was used to mark the TH-positive neurons (green). Scale bars, 75 μm. (E) Bar graph quantitation of the p-α-synuclein level in the ipsilateral substantia nigra. For each treatment, the fluorescence intensity was measured similarly as in (B) with nine mice. Values are presented as mean ± SD. Student's t test, ****$p < 0.0001$,

(legend continued on next page)

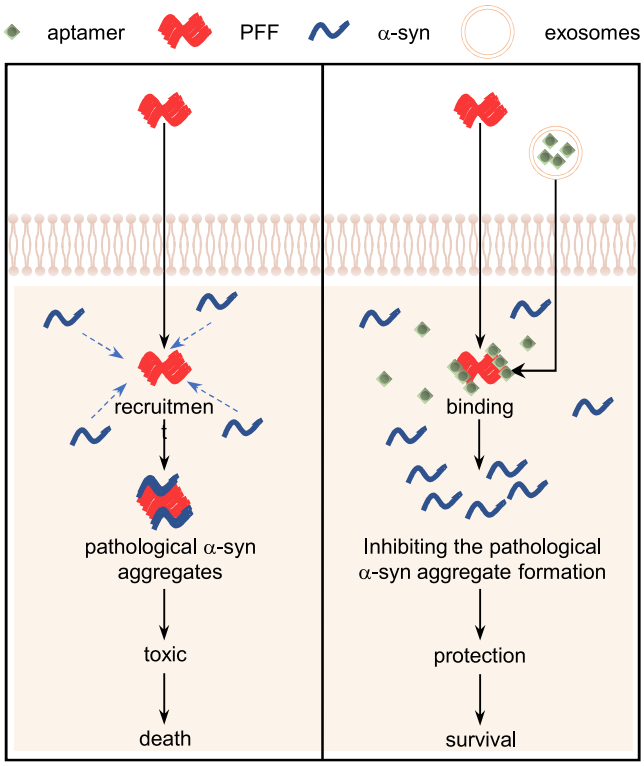

Figure 8. The Aptamers Exerted the Neuroprotective Effects by Retarding PFFs Recruiting Endogenous α-Synuclein into Pathologic Aggregates

The α-synuclein PFF, once taken up by acceptor cells, may act as seeds for further α-synuclein deposition within recipient cells, which triggers the stepwise progression of PD pathology. However, after the aptamers are delivered into the neuronal cells by exosomes, they may block the PFFs recruiting endogenous α-synuclein into pathologic aggregates, consequently preventing synaptic protein loss and mitigating neuron death.

evaluations of the aptamer treatment in mice with the prolonged experimental period.

Although in this study it demonstrated the aptamers could inhibit the intracellular pathological α-synuclein aggregation and could block the Lewy pathology at the very beginning of PD status, the future therapies should rely on early detection of PD by biomarkers such as brain imaging or biological fluid biomarkers currently under development for differential diagnosis.[42] In this way, the aptamer-RVG-exosomes system could be applied at an appropriate intervention time for PD clinical treatment.

In conclusion, by systemic administration of aptamers, we were able to significantly decrease the mouse pathological α-synuclein aggregates in the PD model. This is the first time the aptamer was used successfully *in vivo* to specifically reduce the level of α-synuclein aggregates. These results bolstered the idea that this aptamer-RVG-exosome system could be further developed to abrogate the disease progression in PD, and they further shed light on the clinical treatment of many other CNS diseases, in particular neurodegenerative disorders.

MATERIALS AND METHODS

Preparation of Recombinant α-Synuclein and PFF

The human and mouse α-synuclein genes were respectively subcloned into pGEX-4T-1 vector, and they were expressed in *Escherichia coli* BL21 (DE3) and purified as described previously.[24] After the bacterial endotoxins were removed using the Toxineraser endotoxin removal kit (GeneScript, NJ, USA), the purified α-synuclein protein was diluted in PBS to 5 mg/mL and shaken at 1,000 rpm under 37°C. Seven days later, the protein was centrifuged at 100,000 × *g* for 30 min at 4°C to separate the α-synuclein fibril (pellet fraction) from the α-synuclein monomer (supernatant fraction). The α-synuclein fibril was washed once with PBS and resuspended in PBS to equal volume. The supernatant and pellet were resolved by SDS-PAGE and detected by Coomassie staining. Finally, the PFF and the α-synuclein monomer were respectively aliquoted and stored at −80°C.

Preparation of Aβ42 and Lysozyme Protein Assemblies

Aβ42 oligomers and fibrils were prepared as described previously.[43] At first, Aβ42 (Abcam, Cambridge, UK) was dissolved to 1 mM in 100% hexafluoroisopropanol (HFIP), and HFIP was subsequently removed under vacuum. Then the peptide was resuspended in DMSO to 5 mM. In order to generate oligomeric Aβ42, we added F-12 (without phenol red) culture media to bring the peptide to a final concentration of 100 mM, and the peptide was incubated at 4°C for 24 h. In order to generate fibrillar Aβ42, we added 10 mM HCl to bring the peptide to a final concentration of 100 μM, and the peptide was incubated for 24 h at 37°C. Lysozyme fibrils were prepared as described previously.[44] In brief, lysozyme (MP Biomedicals, Illkirch, France) was dissolved to 10 mg/mL in 10 mM sodium phosphate buffer (pH 7.0) and then incubated at 37°C for 7 days.

Dot Blotting

Proteins (BSA, human monomeric α-synuclein, human α-synuclein PFF, mouse monomeric α-synuclein, mouse α-synuclein PFF; 1 μg each) were respectively immobilized onto the nitrocellulose (NC)

compared with RVG-exosomes group loaded with a random DNA sequence. (F) The activation of microglia and astrocyte was analyzed by confocal microscopy after aptamer treatment. The antibodies of anti-Iba1 and anti-GFAP were used to mark microglia (green) and astrocyte (red), respectively. Scale bars, 75 μm. (G) Bar graph quantitation of Iba-1-positive cells. For each treatment, the number of Iba-1-positive cells was measured with nine mice (three slides per mouse were counted). The number in the aptamer-treated group was normalized to the group treated with a random DNA sequence for statistical comparisons. Values are presented as mean ± SD. Student's t test: n.s., not significant, compared with RVG-exosomes group loaded with a random DNA sequence. (H) Occupied area analyses of GFAP-positive cells. For each treatment, the area occupied by GFAP was measured with nine mice (three slides per mouse were counted). The area in the aptamer-treated group was normalized to the group treated with a random DNA sequence for statistical comparisons. Values are presented as mean ± SD. Student's t test: n.s., not significant, compared with the RVG-exosomes group loaded with a random DNA sequence.

membrane. After blocking with 5% milk in Tris-buffered saline (50 mM Tris, 150 mM NaCl [pH 7.4]) with 0.2% (v/v) Tween-20 (TBST) for 1 h, the membrane was incubated with 100 nM fluorescein isothiocyanate (FITC)-labeled aptamer F5R1 or F5R2 for 2 h at room temperature. Then the membrane was rinsed three times by TBST and incubated with FITC antibody (1:20,000; Huayangzhenglong, Sichuan, China) for 2 h. The membrane was rinsed three times by TBST again and incubated with the rabbit IRDy680 secondary antibody (1:10,000; LI-COR, Lincoln, NE, USA) for 1 h at room temperature. The dots were visualized with Odyssey Infrared Imaging system (LI-COR, Lincoln, NE, USA). Subsequently, blots were stained with Ponceau S (3-hydroxy-4-(2-sulfo-4-[4-sulfophenylazo]phenylazo)-2,7-naphthalenedisulfonic acid; PPLYGEN, Beijing, China) to confirm protein retention.

ThT Fluorescence Assay of α-Synuclein Fibril Formation *In Vitro*

α-Synuclein was dissolved to a concentration of 20 μM in the assembly buffer (50 mM Tris and 150 mM NaCl [pH 7.5]) either alone or with 10% PFF. The mixture was incubated with the aptamer at a 1:1 ratio of PFF at 37°C with constant agitation (1,000 rpm). The samples were collected at the indicated time point, and the rate of fibrillogenesis was monitored by the ThT (20 μM) fluorescence assay (excitation at 450 nm and emission at 480 nm) using a Microplate reader (PerkinElmer, Waltham, MA, USA).

Cell Culture, RVG-Modified Exosomes Isolation, and Aptamer Loading

The human embryonic kidney cell line (HEK293T) and mouse myoblast C2C12cell line were cultured in DMEM with 10% (v/v) fetal bovine serum (FBS), 50 U/mL penicillin, and 50 mg/mL streptomycin. A fast-growing mouse neuroblastoma Neuro2A cell line was cultured in Ham's F-12 Nutrient Mixture (F12) with 10% (v/v) FBS, 50 U/mL penicillin, and 50 mg/mL streptomycin. All of the cells were incubated in a 5% CO_2 atmosphere at 37°C.

The RVG coding sequence was fused to the N terminus of the mouse Lamp2b (as illustrated in Figure S3A). Then, the RVG-Lamp2b (or myc-RVG-lamp2b) plasmids were transfected into HEK293T cells by PEI (Polysciences), and the cells were cultured in exosomes-free DMEM. After 2 days, the medium was collected and RVG-modified exosomes were purified by gradient centrifugation.[32] For aptamer loading, the aptamers (200 pmol) were incubated with PEI (1 mg/mL) in PBS for 30 min; then 10 μg of exosomes was added to the mixture and incubated for the indicated time at 37°C. The excess aptamers and residual PEI were removed by ultracentrifuge at 100,000 × *g* for 90 min at 4°C. The pellet was washed and then resuspended in PBS. For loading efficiency analysis, the fluorescence intensity of Alexa 594 was measured before and after loading aptamer into exosomes by microplate reader (PerkinElmer, Waltham, MA, USA) using 590 nm excitation and 617 nm emission.

Characterization of the RVG-Exosomes

For TEM assay, exosomes (10 μL) were placed on 400-mesh copper grids covered by carbon-stabilized Formvar film (SP I Supplies, West Chester, PA, USA). Two minutes later, the grids were negatively stained with 2% uranyl acetate solution for 5 min at room temperature. Then the grids were rinsed three times with double-distilled H_2O and viewed by a JEM electron microscope (Tokyo, Japan). For biochemical assay, exosomes were lysed in Laemmli buffer, then loaded on a 6%–10% (w/v) SDS-PAGE gel. The proteins were transferred from the gel to polyvinylidene fluoride (PVDF) membranes and blocked with 5% milk. The membranes were incubated with Alix antibody (1:1,000; Abcam, Cambridge, UK) for 2 h at room temperature. After rinsing three times with TBST, the membranes were incubated with the rabbit IRDy680 secondary antibody (1:10,000; LI-COR, Lincoln, NE, USA) for 1 h at room temperature. The bands were visualized using the Odyssey Infrared Imaging system (LI-COR, Lincoln, NE, USA).

Exosomal Staining

Exosomes were stained with CellVue claret far-red fluorescent cell linker kits (Sigma, St. Louis, MO, USA) according to the manufacturer's protocol. In brief, the exosomes were resuspended in the labeling vehicle provided with the kit (Diluent C) to a final concentration of 1 mg/mL. Then the exosomes were rapidly added to 2xDye solution and immediately mixed by pipetting to stain the exosomal membrane. After 5-min incubation at room temperature, the staining was stopped by adding an equal volume of 1% BSA, and the excess dye was removed by ultracentrifuge at 100,000 × *g* for 90 min at 4°C. The exosomes were washed once with PBS and then resuspended in 200 μL of PBS for monitoring the uptake efficiency in cells. The fluorescence intensity of CellVue claret-labeled exosomes was detected by confocal microscope using 655 nm excitation and 675 nm emission.

Primary Neuron Culture and α-Synuclein PFF Treatment

Primary cortex neurons were prepared from C57BL/6J mouse embryos (days 14–16).[24] All experiments were authorized by the Institutional Animal Care and Use Committee of the Capital Medical University (approval No. AEEI-2016-057) and performed according to the NIH *Guide for the Care and Use of Laboratory Animals*. In brief, the dissociated neurons were plated onto the poly-L-lysine (Sigma, St. Louis, MO, USA)-coated coverslips or dishes at 20,000–40,000 or 70,000–100,000 cells/cm^2, respectively. The cells were cultured in Neurobasal medium (GIBCO, VA, USA) supplemented with L-glutamine (0.5 mM) and 50× B27 supplement (for a final concentration of 1×; GIBCO). Because α-synuclein is expressed only at mature synapses, exosome and PFF treatment were performed on neurons at 7 days *in vitro* (DIV). As for the aptamer-loaded RVG-exosomes treatment, 6 μg of the exosomes per 10^6 neurons was used. As for the PFF treatment, the PFF was first diluted in PBS to a final concentration of 0.1 mg/mL and sonicated with 60 pulses. For immunofluorescence experiment, PFF at a final concentration of 1 μg/mL was used. For the immunoblotting experiment, PFF at a final concentration of 4 μg/mL was used. At 21 DIV, the neurons were harvested further to be analyzed.

Immunofluorescence

Neurons or cells were fixed with 4% (w/v) paraformaldehyde and 4% (w/v) sucrose in PBS for 15 min. To extract soluble proteins, we added

1% (v/v) TX-100 to the fix buffer. The cells were rinsed five times with PBS and then permeabilized and blocked with 3% (w/v) BSA/0.1% (v/v) TX-100 for 15 min. Then the cells were incubated with the primary antibody [anti-α-synuclein (1:500; BD Biosciences, Franklin Lakes, NJ, USA) or anti-p-α-synuclein (1:400; Abcam, Cambridge, UK)] for 2 h at room temperature. After rinsing five times with PBS, the cells were incubated with a secondary antibody, mouse IRDy594, rabbit IRDy488, or rabbit IRDy647 (1:500; LI-COR, Lincoln, NE, USA), for 1 h at room temperature. The fluorescence was visualized with confocal microscope (Leica Microsystems, Tokyo, Japan).

Western Blotting

The primary neurons were resuspended in 1% (v/v) TX-100/TBS with protease and phosphatase inhibitors and then sonicated 10 times at a 0.5-s pulse and incubated on ice for 30 min. The cell lysates were centrifuged (100,000 × *g*) at 4°C for 30 min, and the supernatant was harvested as a TX-soluble fraction. The pellets were washed with 1% (v/v) TX-100/TBS followed by centrifugation at 100,000 × *g* at 4°C, and the TX-insoluble proteins were extracted with 2% (w/v) SDS/TBS and finally reconstituted in SDS/TBS buffer with equal volume. The protein concentrations of the TX-soluble fraction and the TX-insoluble fraction were determined using a bicinchoninic acid protein assay kit (Pierce Biotechnology, Rockford, IL, USA). The proteins were resolved by the 6%–15% SDS-PAGE gel and transferred to a PVDF membrane, which was blocked with 5% milk. The membranes were incubated with anti-α-synuclein (1:2,000; BD Biosciences, Franklin Lakes, NJ, USA), anti-β-actin (1:5,000; Beijing GuanXingYu, Beijing, China), anti-p-α-synuclein (1:1,000; Abcam, Cambridge, UK), anti-SNAP25 (1:1,000; ABclonal, Wuhan, China), or anti-synapsin II (homemade, 1:1,000) antibodies for 2 h at room temperature. After rinsing three times with TBST, the membranes were incubated with the secondary antibody, mouse IRDy680 or rabbit IRDy680 (1:10,000; LI-COR, Lincoln, NE, USA), for 1 h at room temperature. The bands were detected with the Odyssey Infrared Imaging system (LI-COR, Lincoln, NE, USA).

Measurement of Cell Viability

Cell viability was determined with the MTT assay. MTT (Promega, Madison, WI, USA) was used at a final concentration of 0.5 mg/mL and incubated with cells for 4 h. After washing two times with PBS, formazan crystals were dissolved in 100 μL DMSO. Absorbance was read at 490 nm with a microplate reader (PerkinElmer, Waltham, MA, USA). The cytotoxicity was measured by the LDH assay, which was carried out using a cytotoxicity detection kit (Roche Diagnostics, Mannheim, Germany). LDH release was measured in a 100-μL aliquot of supernatant, with 100 μL preservation solution used as a blank to correct the optical density reading at 490 nm.

Delivery of Exosomal DNA Aptamer into the Mouse Brain

Two- to three-month-old C57BL/6J female mice were used for experiments. The animals were obtained from Vital River Laboratories (Beijing, China), and all experiments were authorized by the Institutional Animal Care and Use Committee of the Capital Medical University (approval No. AEEI-2016-057) and performed according to the NIH *Guide for the Care and Use of Laboratory Animals*. All animal experiments were designed to minimize the suffering and pain of the animals.

Aptamer-loaded RVG-exosomes (120 μg exosomes per mouse) were administered to the mice by intraperitoneal injection, with random DNA sequence as control. After 24 h, the mice were intrastriatally injected with mouse α-synuclein PFF, which was diluted in sterile PBS to a final concentration of 2.5 mg/mL with brief sonication. In brief, the mice were deeply anesthetized with ketamine (100 mg/kg; Bela-Pharm) and xylazine (10 mg/kg; Bela-Pharm), then were stereotaxically injected with PFF (5 μg) by inserting a single needle into the right dorsal neostriatum (coordinates: +0.2 mm relative to bregma, +2.0 mm from midline, +2.6 mm beneath the dura). Injections were performed using a 10-μL syringe at a rate of 0.1 μL per min (2 μL total per site) with the needle in place for >5 min after injection for a complete absorption of the solution. Sterile PBS was used as negative control; then aptamer-loaded RVG-exosomes were administered to animals weekly by intraperitoneal injection until sacrifice at predetermined period.

Immunohistochemistry

Mice were anesthetized and perfused with physiological saline followed by 4% paraformaldehyde/PBS, and the brains was removed, followed by fixation in 4% paraformaldehyde overnight and transfer to 30% sucrose for cryoprotection. Then the brains were sectioned at a thickness of 40 μm, and the sections were incubated in 0.3% TX-100/PBS for 60 min and then incubated in 3% H_2O_2 for 10 min to block endogenous peroxidase activity. After washing in PBS, sections were incubated in 10% goat serum followed by 0.1% TX-100 in PBS for 60 min, then incubated in anti-tyrosine hydroxylase (TH) (1:8,000; Sigma, St. Louis, MO, USA), anti-p-α-synuclein (1:400; Abcam, Cambridge, UK), anti-MAP2 (1:400; Abcam, Cambridge, UK), anti-GFAP (1:400; Abcam, Cambridge, UK), or anti-Iba1 (1:200; Wako Pure Chemical Industries, Japan) antibodies for 2 h at room temperature. After washing in PBS, the brain slices were incubated with secondary antibody, mouse IRDy594 or rabbit IRDy488 (1:500; LI-COR, Lincoln, NE, USA), for 1 h at room temperature. The fluorescence was visualized and analyzed with confocal microscope (Leica Microsystems, Tokyo, Japan).

Behavioral Analysis

Behavioral experiments were conducted 30 days post PFF injection. Mice were habituated to the testing room 1 h before tests, and the apparatuses were cleaned with 70% ethanol in between animals to minimize odor cues. For rotarod test, each mouse was given a training session (four 5-min trials, 5 min apart) to acclimate them to the rotarod apparatus. During the test period, each mouse was placed on the rotarod with increasing speed, from 4 to 40 rpm in 300 s. The latency to fall off the rotarod within this time period was recorded. Each mouse received two consecutive trials, and the mean latency to fall in each group was used in the analysis. For the wire hang test, it was conducted with a modified protocol previously described.[45] The mice

were placed on the top of a standard wire cage lid. The lid was lightly shaken to cause the animals to grip the wires and then turned upside down. The latency of mice to fall off the wire grid was measured, and average values were computed from two trials (15 min apart). Trials were stopped if the mouse remained on the lid after 15 min. For each group, we used 12 female mice for behavioral analysis.

Statistical Analysis

The statistical analysis was completed using GraphPad Prism software (version 6; GraphPad, La Jolla, CA, USA). Data results are presented as mean ± SD with at least three independent experiments. Differences between two means and among multiple means were assessed by unpaired two-tailed Student's t test or ANOVA followed by Tukey's post hoc test, respectively. Assessments with $p < 0.05$ were considered statistically significant.

SUPPLEMENTAL INFORMATION

Supplemental Information can be found online at https://doi.org/10.1016/j.omtn.2019.07.008.

AUTHOR CONTRIBUTIONS

J.Z. designed the experiments and wrote the paper; X.R., Y. Zhao., and F.X. conducted experiments; Y. Zheng and H.H. analyzed the data; W.W., Y.C., and H.Y. made constructive suggestions for this experiment and interpreted the data.

CONFLICTS OF INTEREST

The authors declare no competing interests.

ACKNOWLEDGMENTS

This work was supported by grants from the National Natural Science Foundation of China (31571202 and 31271136), Beijing Municipal Natural Science Foundation (7192018), and Importation and Development of High-Caliber Talents Project of Beijing Municipal Institutions (CIT&TCD201504087).

REFERENCES

1. Jellinger, K.A. (2003). Neuropathological spectrum of synucleinopathies. Mov. Disord. *18* (*Suppl 6*), S2–S12.
2. Brundin, P., Atkin, G., and Lamberts, J.T. (2015). Basic science breaks through: New therapeutic advances in Parkinson's disease. Mov. Disord. *30*, 1521–1527.
3. Iwai, A., Masliah, E., Yoshimoto, M., Ge, N., Flanagan, L., de Silva, H.A., Kittel, A., and Saitoh, T. (1995). The precursor protein of non-A beta component of Alzheimer's disease amyloid is a presynaptic protein of the central nervous system. Neuron *14*, 467–475.
4. Spillantini, M.G., Schmidt, M.L., Lee, V.M., Trojanowski, J.Q., Jakes, R., and Goedert, M. (1997). Alpha-synuclein in Lewy bodies. Nature *388*, 839–840.
5. Bergström, A.L., Kallunki, P., and Fog, K. (2016). Development of Passive Immunotherapies for Synucleinopathies. Mov. Disord. *31*, 203–213.
6. Wu, K.P., Weinstock, D.S., Narayanan, C., Levy, R.M., and Baum, J. (2009). Structural reorganization of alpha-synuclein at low pH observed by NMR and REMD simulations. J. Mol. Biol. *391*, 784–796.
7. Valera, E., and Masliah, E. (2016). Combination therapies: The next logical Step for the treatment of synucleinopathies? Mov. Disord. *31*, 225–234.
8. Valera, E., Spencer, B., and Masliah, E. (2016). Immunotherapeutic Approaches Targeting Amyloid-β, α-Synuclein, and Tau for the Treatment of Neurodegenerative Disorders. Neurotherapeutics *13*, 179–189.
9. Frydman-Marom, A., Shaltiel-Karyo, R., Moshe, S., and Gazit, E. (2011). The generic amyloid formation inhibition effect of a designed small aromatic β-breaking peptide. Amyloid *18*, 119–127.
10. He, Q., Koprich, J.B., Wang, Y., Yu, W.B., Xiao, B.G., Brotchie, J.M., and Wang, J. (2016). Treatment with Trehalose Prevents Behavioral and Neurochemical Deficits Produced in an AAV α-Synuclein Rat Model of Parkinson's Disease. Mol. Neurobiol. *53*, 2258–2268.
11. Takahashi, M., Suzuki, M., Fukuoka, M., Fujikake, N., Watanabe, S., Murata, M., Wada, K., Nagai, Y., and Hohjoh, H. (2015). Normalization of Overexpressed α-Synuclein Causing Parkinson's Disease By a Moderate Gene Silencing With RNA Interference. Mol. Ther. Nucleic Acids *4*, e241.
12. Bae, E.J., Lee, H.J., Rockenstein, E., Ho, D.H., Park, E.B., Yang, N.Y., Desplats, P., Masliah, E., and Lee, S.J. (2012). Antibody-aided clearance of extracellular α-synuclein prevents cell-to-cell aggregate transmission. J. Neurosci. *32*, 13454–13469.
13. Masliah, E., Rockenstein, E., Adame, A., Alford, M., Crews, L., Hashimoto, M., Seubert, P., Lee, M., Goldstein, J., Chilcote, T., et al. (2005). Effects of alpha-synuclein immunization in a mouse model of Parkinson's disease. Neuron *46*, 857–868.
14. Masliah, E., Rockenstein, E., Mante, M., Crews, L., Spencer, B., Adame, A., Patrick, C., Trejo, M., Ubhi, K., Rohn, T.T., et al. (2011). Passive immunization reduces behavioral and neuropathological deficits in an alpha-synuclein transgenic model of Lewy body disease. PLoS ONE *6*, e19338.
15. Sevigny, J., Chiao, P., Bussière, T., Weinreb, P.H., Williams, L., Maier, M., Dunstan, R., Salloway, S., Chen, T., Ling, Y., et al. (2016). The antibody aducanumab reduces Aβ plaques in Alzheimer's disease. Nature *537*, 50–56.
16. Boutajangout, A., Ingadottir, J., Davies, P., and Sigurdsson, E.M. (2011). Passive immunization targeting pathological phospho-tau protein in a mouse model reduces functional decline and clears tau aggregates from the brain. J. Neurochem. *118*, 658–667.
17. Yanamandra, K., Kfoury, N., Jiang, H., Mahan, T.E., Ma, S., Maloney, S.E., Wozniak, D.F., Diamond, M.I., and Holtzman, D.M. (2013). Anti-tau antibodies that block tau aggregate seeding in vitro markedly decrease pathology and improve cognition in vivo. Neuron *80*, 402–414.
18. Gros-Louis, F., Soucy, G., Larivière, R., and Julien, J.P. (2010). Intracerebroventricular infusion of monoclonal antibody or its derived Fab fragment against misfolded forms of SOD1 mutant delays mortality in a mouse model of ALS. J. Neurochem. *113*, 1188–1199.
19. Wolfgang, W.J., Miller, T.W., Webster, J.M., Huston, J.S., Thompson, L.M., Marsh, J.L., and Messer, A. (2005). Suppression of Huntington's disease pathology in Drosophila by human single-chain Fv antibodies. Proc. Natl. Acad. Sci. USA *102*, 11563–11568.
20. Qu, J., Yu, S., Zheng, Y., Zheng, Y., Yang, H., and Zhang, J. (2017). Aptamer and its applications in neurodegenerative diseases. Cell. Mol. Life Sci. *74*, 683–695.
21. Rhie, A., Kirby, L., Sayer, N., Wellesley, R., Disterer, P., Sylvester, I., Gill, A., Hope, J., James, W., and Tahiri-Alaoui, A. (2003). Characterization of 2′-fluoro-RNA aptamers that bind preferentially to disease-associated conformations of prion protein and inhibit conversion. J. Biol. Chem. *278*, 39697–39705.
22. Sayer, N.M., Cubin, M., Rhie, A., Bullock, M., Tahiri-Alaoui, A., and James, W. (2004). Structural determinants of conformationally selective, prion-binding aptamers. J. Biol. Chem. *279*, 13102–13109.
23. Rahimi, F. (2018). Aptamers Selected for Recognizing Amyloid β-Protein-A Case for Cautious Optimism. Int. J. Mol. Sci. *19*, e668.
24. Zheng, Y., Qu, J., Xue, F., Zheng, Y., Yang, B., Chang, Y., Yang, H., and Zhang, J. (2018). Novel DNA Aptamers for Parkinson's Disease Treatment Inhibit α-Synuclein Aggregation and Facilitate its Degradation. Mol. Ther. Nucleic Acids *11*, 228–242.
25. Cocucci, E., Racchetti, G., and Meldolesi, J. (2009). Shedding microvesicles: artefacts no more. Trends Cell Biol. *19*, 43–51.

26. Zhang, Y., Li, L., Yu, J., Zhu, D., Zhang, Y., Li, X., Gu, H., Zhang, C.Y., and Zen, K. (2014). Microvesicle-mediated delivery of transforming growth factor β1 siRNA for the suppression of tumor growth in mice. Biomaterials *35*, 4390–4400.

27. Zhang, Y., Liu, D., Chen, X., Li, J., Li, L., Bian, Z., Sun, F., Lu, J., Yin, Y., Cai, X., et al. (2010). Secreted monocytic miR-150 enhances targeted endothelial cell migration. Mol. Cell *39*, 133–144.

28. van den Boorn, J.G., Schlee, M., Coch, C., and Hartmann, G. (2011). SiRNA delivery with exosome nanoparticles. Nat. Biotechnol. *29*, 325–326.

29. Wrzesinski, S.H., Wan, Y.Y., and Flavell, R.A. (2007). Transforming growth factor-beta and the immune response: implications for anticancer therapy. Clin. Cancer Res. *13*, 5262–5270.

30. Alvarez-Erviti, L., Seow, Y., Yin, H., Betts, C., Lakhal, S., and Wood, M.J. (2011). Delivery of siRNA to the mouse brain by systemic injection of targeted exosomes. Nat. Biotechnol. *29*, 341–345.

31. Liu, Y., Li, D., Liu, Z., Zhou, Y., Chu, D., Li, X., Jiang, X., Hou, D., Chen, X., Chen, Y., et al. (2015). Targeted exosome-mediated delivery of opioid receptor Mu siRNA for the treatment of morphine relapse. Sci. Rep. *5*, 17543.

32. Cooper, J.M., Wiklander, P.B., Nordin, J.Z., Al-Shawi, R., Wood, M.J., Vithlani, M., Schapira, A.H., Simons, J.P., El-Andaloussi, S., and Alvarez-Erviti, L. (2014). Systemic exosomal siRNA delivery reduced alpha-synuclein aggregates in brains of transgenic mice. Mov. Disord. *29*, 1476–1485.

33. Luk, K.C., Kehm, V., Carroll, J., Zhang, B., O'Brien, P., Trojanowski, J.Q., and Lee, V.M. (2012). Pathological α-synuclein transmission initiates Parkinson-like neurodegeneration in nontransgenic mice. Science *338*, 949–953.

34. Fares, M.B., Maco, B., Oueslati, A., Rockenstein, E., Ninkina, N., Buchman, V.L., Masliah, E., and Lashuel, H.A. (2016). Induction of de novo α-synuclein fibrillization in a neuronal model for Parkinson's disease. Proc. Natl. Acad. Sci. USA *113*, E912–E921.

35. Krebs, M.R., Bromley, E.H., and Donald, A.M. (2005). The binding of thioflavin-T to amyloid fibrils: localisation and implications. J. Struct. Biol. *149*, 30–37.

36. Volpicelli-Daley, L.A., Luk, K.C., Patel, T.P., Tanik, S.A., Riddle, D.M., Stieber, A., Meaney, D.F., Trojanowski, J.Q., and Lee, V.M. (2011). Exogenous α-synuclein fibrils induce Lewy body pathology leading to synaptic dysfunction and neuron death. Neuron *72*, 57–71.

37. Tran, H.T., Chung, C.H., Iba, M., Zhang, B., Trojanowski, J.Q., Luk, K.C., and Lee, V.M. (2014). A-synuclein immunotherapy blocks uptake and templated propagation of misfolded α-synuclein and neurodegeneration. Cell Rep. *7*, 2054–2065.

38. Irwin, D.J., White, M.T., Toledo, J.B., Xie, S.X., Robinson, J.L., Van Deerlin, V., Lee, V.M., Leverenz, J.B., Montine, T.J., Duda, J.E., et al. (2012). Neuropathologic substrates of Parkinson disease dementia. Ann. Neurol. *72*, 587–598.

39. Luk, K.C., Kehm, V.M., Zhang, B., O'Brien, P., Trojanowski, J.Q., and Lee, V.M. (2012). Intracerebral inoculation of pathological α-synuclein initiates a rapidly progressive neurodegenerative α-synucleinopathy in mice. J. Exp. Med. *209*, 975–986.

40. Johnsen, K.B., Gudbergsson, J.M., Skov, M.N., Pilgaard, L., Moos, T., and Duroux, M. (2014). A comprehensive overview of exosomes as drug delivery vehicles - endogenous nanocarriers for targeted cancer therapy. Biochim. Biophys. Acta *1846*, 75–87.

41. Tian, Y., Li, S., Song, J., Ji, T., Zhu, M., Anderson, G.J., Wei, J., and Nie, G. (2014). A doxorubicin delivery platform using engineered natural membrane vesicle exosomes for targeted tumor therapy. Biomaterials *35*, 2383–2390.

42. Eller, M., and Williams, D.R. (2009). Biological fluid biomarkers in neurodegenerative parkinsonism. Nat. Rev. Neurol. *5*, 561–570.

43. Dahlgren, K.N., Manelli, A.M., Stine, W.B., Jr., Baker, L.K., Krafft, G.A., and LaDu, M.J. (2002). Oligomeric and fibrillar species of amyloid-beta peptides differentially affect neuronal viability. J. Biol. Chem. *277*, 32046–32053.

44. Morozova-Roche, L.A., Zurdo, J., Spencer, A., Noppe, W., Receveur, V., Archer, D.B., Joniau, M., and Dobson, C.M. (2000). Amyloid fibril formation and seeding by wild-type human lysozyme and its disease-related mutational variants. J. Struct. Biol. *130*, 339–351.

45. Santa-Maria, I., Diaz-Ruiz, C., Ksiezak-Reding, H., Chen, A., Ho, L., Wang, J., and Pasinetti, G.M. (2012). GSPE interferes with tau aggregation in vivo: implication for treating tauopathy. Neurobiol. Aging *33*, 2072–2081.

OMTN, Volume *17*

Supplemental Information

Exosomal DNA Aptamer Targeting α-Synuclein Aggregates Reduced Neuropathological Deficits in a Mouse Parkinson's Disease Model

Xiaoxi Ren, Yun Zhao, Fenqin Xue, Yan Zheng, Haixia Huang, Wei Wang, Yongchang Chang, Hui Yang, and Jianliang Zhang

SUPPLEMENTARY MATERIALS

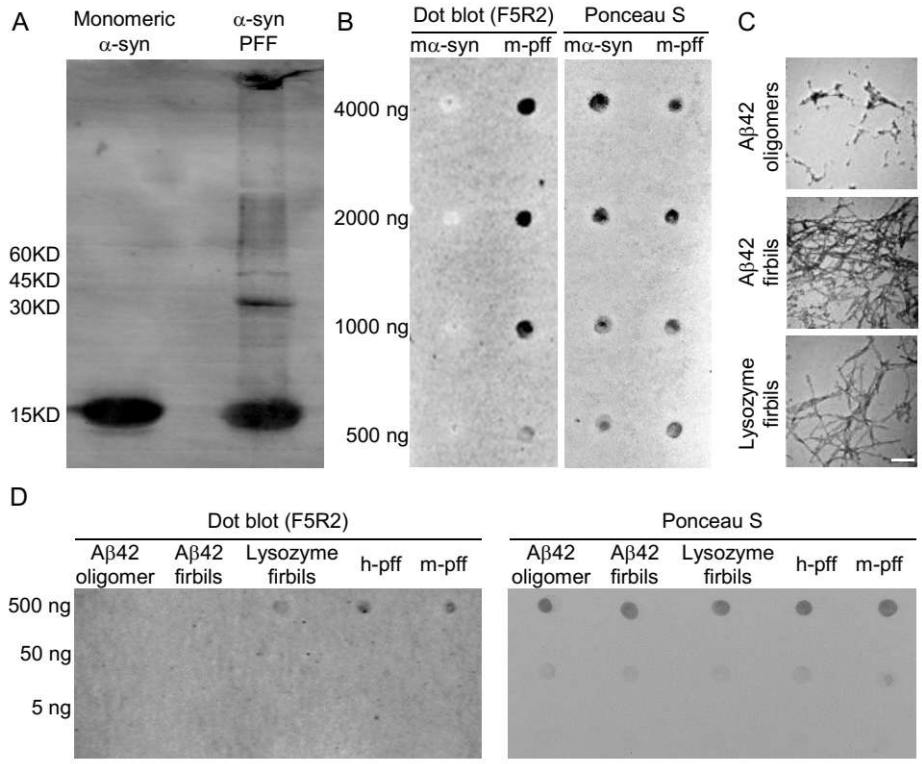

Figure S1. Analysis of the specificity of the aptamer F5R2. (**A**) The α-synuclein PFF was prepared in PBS with constant agitation. After the α-synuclein fibril (pellet fraction) was separated from the α-synuclein monomer (supernatant fraction) by ultracentrifuge, the proteins were detected by western blot with anti-α-synuclein (BD Biosciences, 1:2000). (**B**) Aptamer recognition capability assay by dot blotting. Monomeric and fibrillar mouse α- synuclein were spotted at 500 ng, 1000 ng, 2000 ng and 4000 ng and membranes were probed with FITC labeled aptamer F5R2. Blots were stained with Ponceau S after probing and washing to confirm protein retention. (**C**) Electron micrographs of Aβ42 oligomers, Aβ42 firbils and lysozyme firbils. Scale bar, 200 nm. (**D**) Reactivity of aptamer F5R2 with different amyloid fibrils. Aβ42 oligomers, Aβ42 firbils and lysozyme firbils were spotted (1 μL) onto NC membranes and probed with FITC-labeled aptamer F5R2. h-pff and m-pff were used as positive controls. Blots were stained with Ponceau S after probing and washing to confirm protein retention.

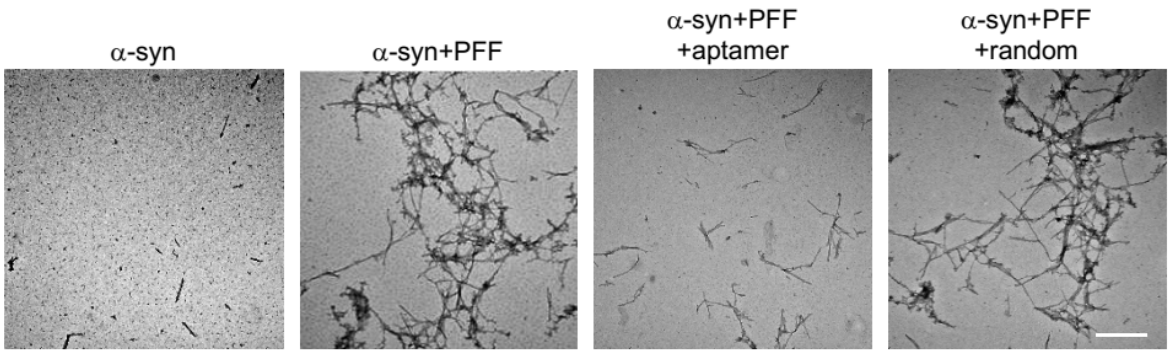

Figure S2. Aptamer F5R2 could inhibit PFF-induced aggregation procession *in vitro*. The human α-synuclein monomer (20 μM) was incubated with 10% PFF in the presence or absence of aptamer F5R2 (2 μM) at 37 °C under shaking at 1000 rpm. After shaking for 24 hours, amyloid formation was monitored by TEM. Sacle bar, 500 nm.

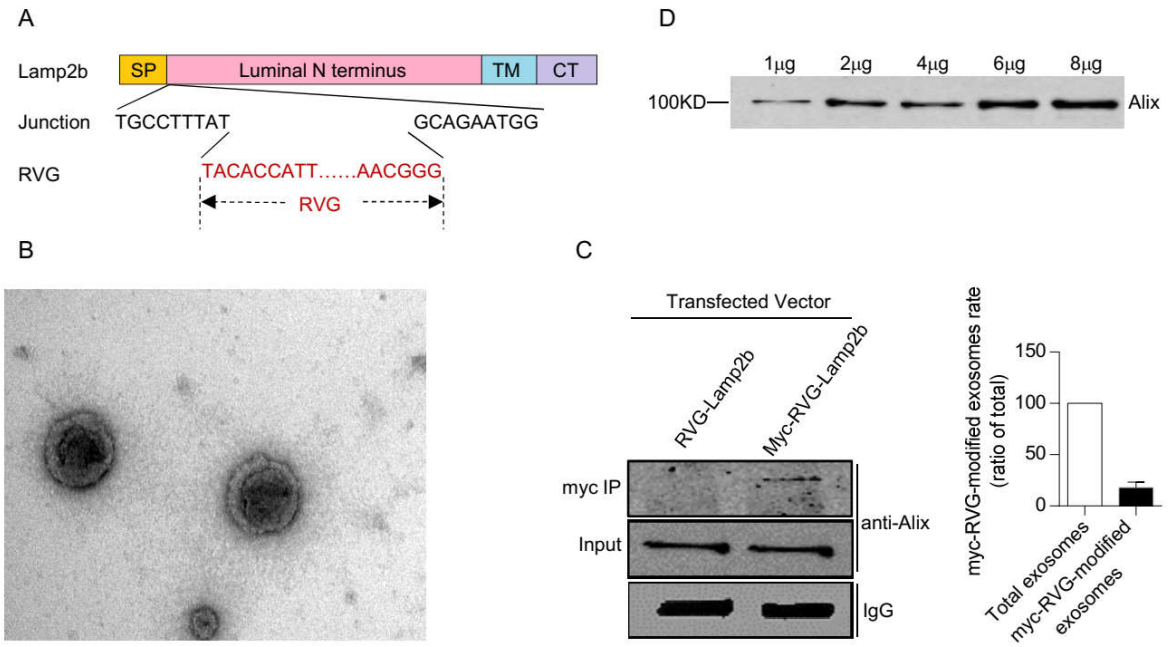

Figure S3. Schematic representation of RVG-Lamp2b cloning and characterization of the RVG-exosomes. (**A**) The RVG peptide was cloned into the N-terminus of Lamp2b. SP, signal peptide; TM, transmembrane domain; CT, C terminus. (**B**) The protein of Alix, marker of exosomes, was detected in the samples from the RVG-exosome lysates by western blotting. (**C**) The plasmids encoding myc-RVG-lamp2b were transfected into HEK 293Tcells for 48 h before exosomes were collected. Plasmids encoding RVG-lamp2b were used as negative control. The ratio of myc-RVG-positive exosomes to total ones was assessed by IP/Western blot analysis. Histograms show average densitometry values of Alix from immunoprecipitated and total fraction. (**D**) TEM image of the RVG-exosomes loaded with aptamers. Bar=200 nm.

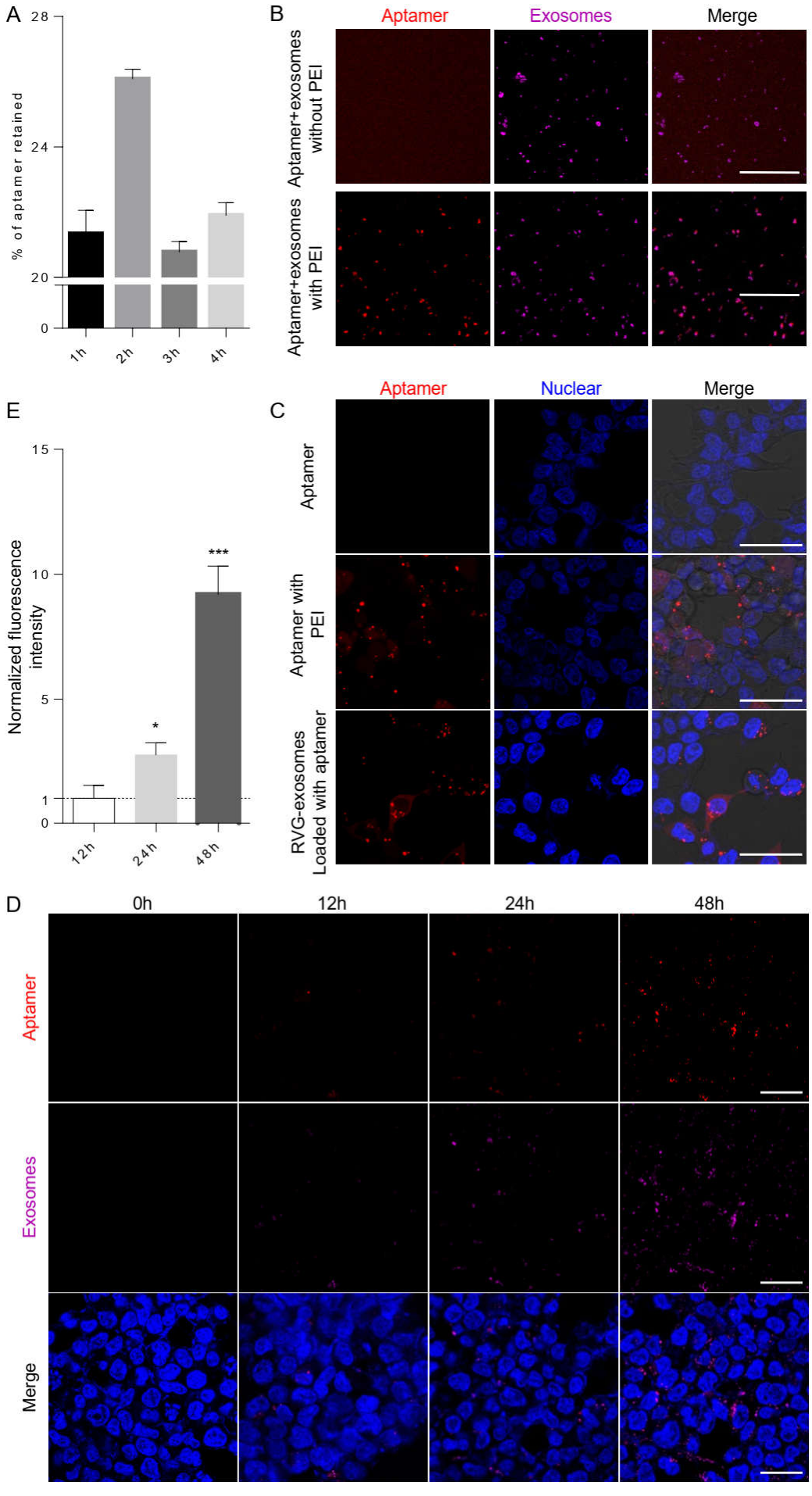
A
% of aptamer retained
28
24
20
0
1h
2h
3h
4h
B
Aptamer
Exosomes
Merge
Aptamer+exosomes without PEI
Aptamer+exosomes with PEI
E
Normalized fluorescence intensity
15
10
5
1
0
*
***
12h
24h
48h
C
Aptamer
Nuclear
Merge
Aptamer
Aptamer with PEI
RVG-exosomes Loaded with aptamer
D
0h
12h
24h
48h
Aptamer
Exosomes
Merge

Figure S4. Aptamer F5R2 was loaded into exosomes by polyethylenimine transfection. (**A**) RVG-exosomes stained with CellVue Claret were incubated with Alexa 594 labeled aptamer F5R2 for different times (1, 2, 3 and 4 hours) in the presence of polyethylenimine (PEI). After the exosomes were harvested with 100,000g for 1 hour, they were resuspended in the PBS and the aptamer fluorescence was assayed on the fluorescent plate reader. n=6. (**B**) After RVG-exosomes stained with CellVue Claret were incubated with Alexa 594 labeled aptamer F5R2 for 2 hours in the presence of polyethylenimine, the pelleted exosomes and aptamers were co-visualized by confocal microscopy, with non-transfection-treated group as negative control. Bar=50 μm. (**C**) Neuro2A cells were incubated with naked aptamers or the RVG-exosomes loaded with aptamers for 24h. The mixture of transfection reagent (PEI) and aptamers was used as a positive control. Confocal images was used to measure the delivery efficiency of different approaches. (**D**) The RVG-exosomes loaded with aptamers were incubated with Neuro2A cells for 0,12, 24 and 48 hours, and then the cells were washed by PBS for three times. Confocal micrograph was used to detect the fluorescence of Alexa594-labeled aptamers (Red) and exosomes (Purple). Bar=50 μm. (**E**) Quantitative analyses of fluorescence intensity of aptamers at 12, 24 and 48h. Values are presented as mean ± SD. One-way ANOVA followed by Tukey's post hoc test (n=3 per group), *$p<0.05$, ***$p < 0.001$ compared with the group that was treated for 12h.

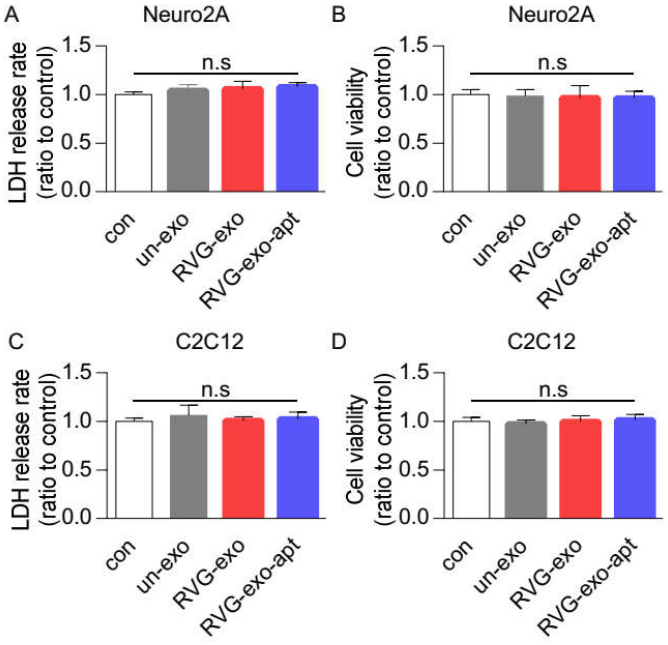

Figure S5. Treatment with aptamer-loaded exosomes was tolerated by cells. LDH assay (**A, C**) and MTT assay (**B, D**) were performed 24 hours after Neuro2A and C2C12 cells were incubated with naked aptamers (con), unmodified exosomes (un-exo), RVG-exosomes (RVG-exo) and RVG-exosomes loaded with aptamer F5R2 (RVG-exo-apt). Values are presented as mean ± SD. One-way ANOVA followed by Tukey's post hoc test (n=6 per group), n.s: not significant.

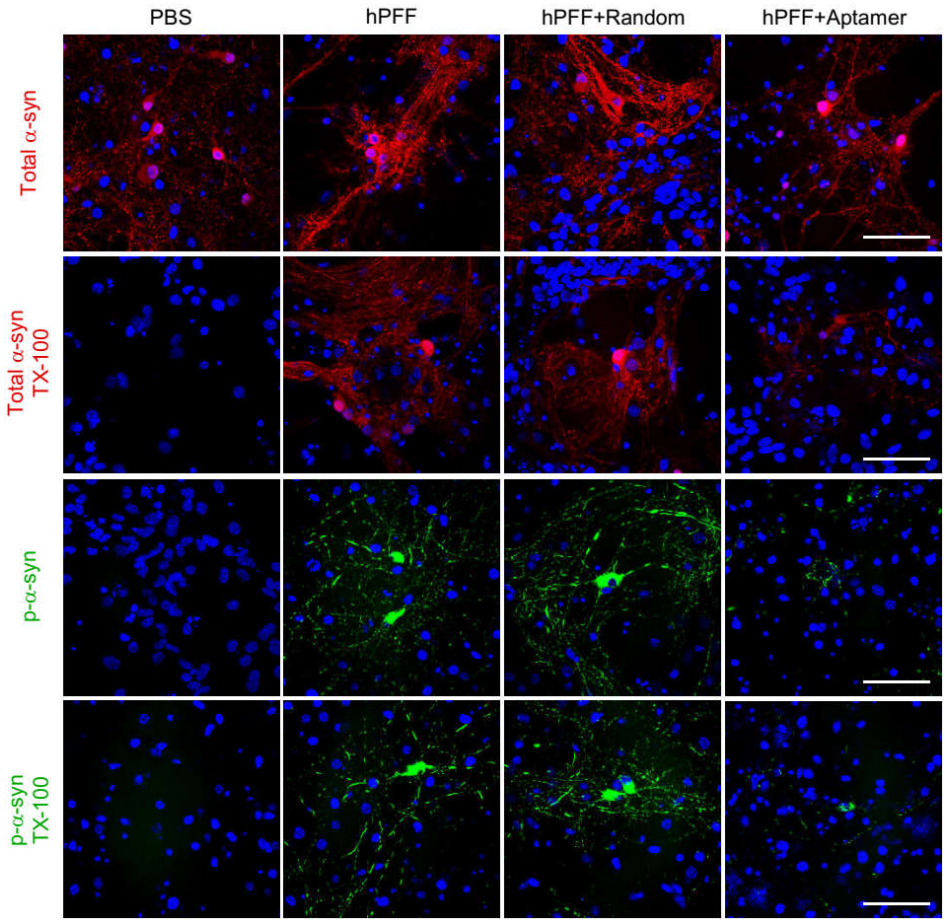

Figure S6. Confocal microscope images in Figure 3A were merged with DAPI blue to show cell density.

Scale bar, 25 mm.

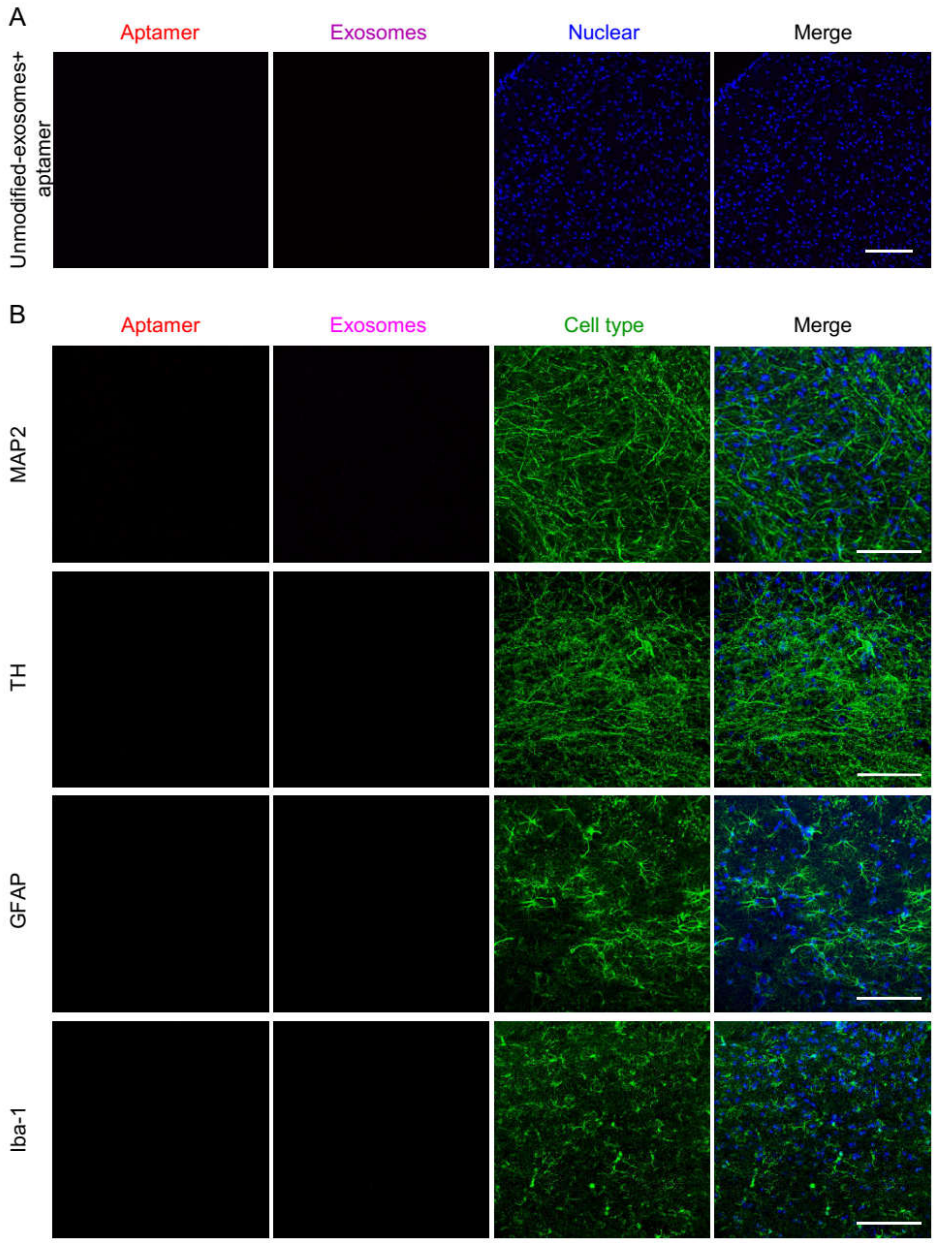

Figure S7. Unmodified exosomes could hardly deliver aptamers into the central nervous system in mice. Unmodified-exosomes were labeled, loaded and administered as described in Figure 5. Twenty-four hours later, mice were sacrificed, perfused, and brain slides were subjected for confocal examinations. Little, if any, of the red aptamer signals were detectable in the brain cortex (**A**) and midbrain (**B**). Brain slides were stained with antibodies (anti-MAP2, anti-TH, anti-GFAP and anti-Iba-1) to different cell types. Scale bar, 75 μm.

Supplementary Table 1. Plasm cytokine concentrations (pg/ml) in mice after aptamer treatment

	Control	aptamer-RVG exosomes	aptamer-exosomes	aptamer-PEI
IL-6	32.63(±2.06)	36.61（±2.59）	38.12(±1.98)	49.57(±1.85)**
IFN-α	14.75(±2.24)	15.60(±3.92)	15.84(±3.67)	18.30(±2.19)*
IP-10	46.79(±3.68)	48.98(±4.60)	50.40(±6.39)	54.53(±5.83)*
TNF-α	226.64(±22.78)	240.44(±16.11)	233.48(±33.75)	323.27(±46.07)*